

SESSION 4A

WESTERN GAS RESEARCH

SYSTEMS ANALYSIS OF LOW PERMEABILITY NATURAL GAS FORMATIONS

1. CONTRACT NUMBER: 896 (UNCONVENTIONAL GAS)

CONTRACTOR: DOE/METC/STS Division
PO Box 880
Morgantown, WV 26507
(304) 291-4217

CONTRACTOR PROGRAM MANAGER: N/A

PRINCIPAL INVESTIGATOR: John Duda

METC PROJECT MANAGER: K-H Frohne

CONTRACT PERIOD OF PERFORMANCE: October 1, 1988 through
September 30, 1989

2. SCHEDULE/MILESTONES:

FISCAL YEAR 89 PROJECT SCHEDULE

	O	N	D	J	F	M	A	M	J	J	A	S
Develop horizontal well production type curves												
Update geologic data base for the Washakie basin												
Compile/analyze permeability data for the Washakie basin												
Sensitivity analysis of gas reserves												
Initial appraisal of "extrapolated" areas												

3. OBJECTIVES:

Systems analysis of unconventional natural gas at the Morgantown Energy Technology Center (METC) focuses on two broad objectives: 1) develop estimates of recoverable gas from low permeability formations, and 2) define "least cost" strategies for exploitation of the resource. In addition to these principal objectives, other goals of the project are to investigate the sensitivity of natural gas reserves to improved extraction technologies and to help guide future research efforts. Guidance of future research direction will be supported through the identification of technologies which indicate significant reserve-base increases. The project objectives are being realized using an integrated gas resources model (ICF-Lewin Energy 1988). The model couples geologic descriptions, production technologies, and financial aspects

of "tight gas" formations to generate estimates of economically recoverable gas.

4. BACKGROUND STATEMENT:

Several groups have developed estimates of in-place and recoverable gas volumes from low permeability sources (Supply-Technical Advisory Task Force 1978, Kuuskraa, et al. 1978, National Petroleum Council 1980). Probably the most widely publicized study of unconventional gas sources is the National Petroleum Council's (NPC) study. The Council estimated 192 trillion cubic feet (Tcf) of recoverable gas for the lower 48 using a "current technology" scenario and a gas price of \$2.50/thousand cubic feet (Mcf). These 1980 estimates were determined by analyzing basins and other low permeability gas prone areas throughout the United States. The Council's basin-level analysis resulted in an in-place gas volume of 136 Tcf for the Greater Green River basin with 3.1 Tcf recoverable (current technology, \$2.50/Mcf, 15% discounted cash flow rate of return (DCFROR)).

More recently, the United States Geological Survey (USGS) reported a resource base of 4,971 Tcf for the Greater Green River basin with 73 Tcf recoverable (base technology, \$5.00/Mcf) (United States Geological Survey 1988). Many reasons exist for the differences between the NPC's and the USGS's estimates including study methodology, and the areal and vertical extent of the formations considered in the investigations. The NPC explicitly addressed production technology in their study; hydraulic fracture lengths, etc. were quantified. The USGS also considered current and advanced technologies in their study, but in a qualitative sense. The USGS defined "current technology" as present state-of-the-art drilling and completion procedures and "advanced technology" as greatly improved recovery methods.

The USGS has studied low permeability natural gas formations, in part, to provide data and other support research for high-quality reserve assessments. Much of the USGS's research has targeted Rocky Mountain basins which have considerable natural gas potential. Their work has also led to new insights concerning the generation and occurrence of overpressured gas in these sedimentary basins (Spencer 1985). For example, in deeper, organic-rich parts of several Rocky Mountain basins, gas continues to be generated at a faster rate than it can escape, resulting in pressures greater than hydrostatic. In addition, many natural gas reservoirs occur downdip of water-bearing sandstones due to updip "relative permeability to gas barriers."

The Department of Energy (DOE) has identified three western basins as "priority" study areas. These basins are the Greater Green River basin, the Piceance basin, and the Uinta basin. These basins have been selected by DOE as priority research targets because of their significant resource potential and the many technical and economic questions blocking industry development of the resource (Morgantown Energy Technology Center 1987). Table 1 shows the NPC's and the USGS's estimates of natural gas for DOE's priority basins.

In past studies, the resource potential for some areas was developed through the extrapolation of more quantified data. The eastern region in the NPC's study is one example in which "surrogate", appraised formations were used to represent formations that were not appraised. Figure 1 illustrates the

extrapolation methodology used for the NPC's eastern region. Considerable data have been generated during the last 10 years for these extrapolated areas. Inclusion of this previously unavailable information will allow a more definitive assessment of these select areas.

Table 1. Comparison of the NPC and USGS estimates of tight gas potential.

<u>Basin</u>	DOE "Priority" Basins			
	<u>1980 NPC^{1,3}</u>		<u>1987-88 USGS^{2,3}</u>	
	GIP	Recoverable ⁴	GIP	Recoverable ⁵
Greater Green River	136	3.1	4,971	73.4
Piceance	49	12.9	420	13.4
Uinta	20	12.2	20	13.9 ⁶
Totals	205	28.2	5,411	100.7

- 1) National Petroleum Council
- 2) United States Geological Survey
- 3) trillions of cubic feet (Tcf)
- 4) base technology, \$2.50/Mcf, 15% DCFROR
- 5) current technology, \$5/Mcf
- 6) USGS mod. of 1980 NPC estimate

5. PROJECT DESCRIPTION:

The systems effort at METC is a series of subtasks that will collectively lead to new estimates of economically recoverable gas from low permeability formations. The effort integrates information generated, measured, and interpreted through other research studies in order to assess the potential of tight gas sands. The information includes new geological interpretations of tight gas settings, recovery efficiencies of improved production technologies, and updated capital and operating costs.

The Greater Green River basin is the largest of the priority basins in terms of areal extent and has considerable natural gas potential. As shown in Table 1, estimates of recoverable gas range considerably. Updated descriptions of stratigraphy, structure, and reservoir properties are being developed into a data base for use in the systems model. Initially, estimates of recoverable gas will be developed for subbasins within the Greater Green River basin. The first subarea being reviewed is the Washakie basin which is located east of the Rock Springs uplift. Published correlations of the low permeability horizons underlying this area are being used to establish the areal and vertical extent of the reservoirs (Tyler 1978). Estimates of gas-in-place and determinations of reservoir quality will be generated from

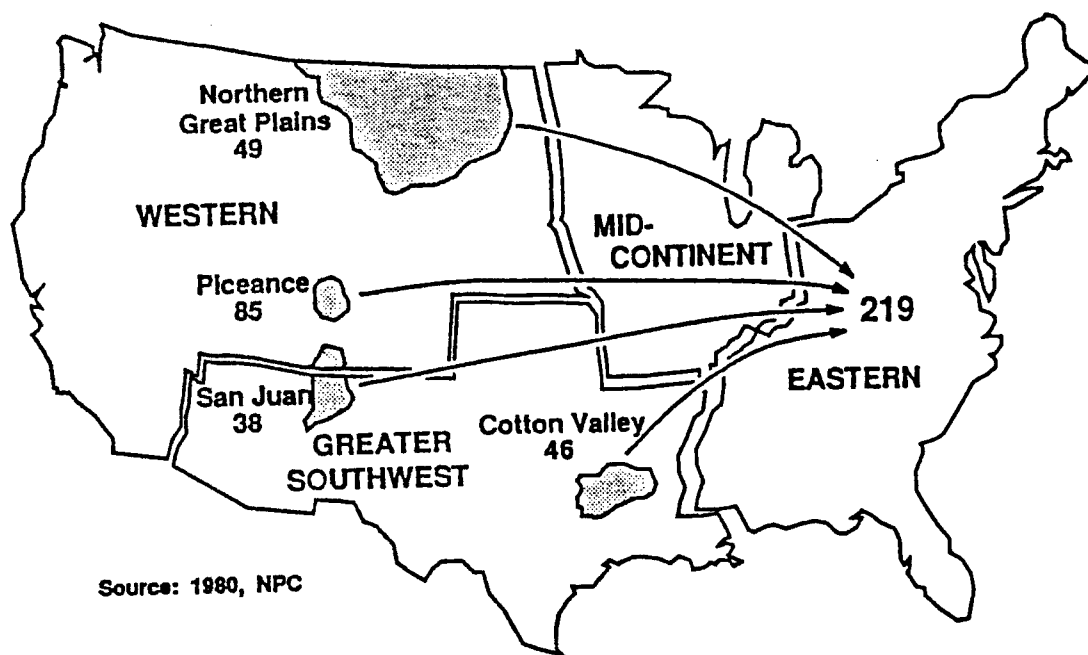


Figure 1. Extrapolated gas estimate for the NPC's eastern region.

the cross-sections and other well logs. Figure 2 shows the Washakie study area (Law, et al. 1987).

The Clinton sandstone is one eastern formation being appraised in terms of recoverable gas. The sand underlies NE Ohio and extends into neighboring states. Figure 3 shows the presently drilled portion of the Clinton sand (EG&G 1988). The Clinton is a subset of the formations which comprise the eastern region in the NPC study. Estimates of recoverable gas were extrapolated from other, appraised formations in that study. For example, the eastern region was represented by formations from the Piceance and San Juan basins, the Cotton Valley sand underlying east Texas, and gas-bearing rocks underlying the Northern Great Plains area. Reservoir properties are being compiled and structured for use in the systems model. Once this task is complete, estimates of natural gas potential will be prepared for the Clinton sand.

Permeability is a necessary, but elusive, reservoir property that must be quantified in the systems model in order to evaluate alternative production technologies. Core analysis or pressure transient methods are generally used to evaluate reservoir permeability. These procedures increase well costs which preclude them from being completed on a routine basis. A commercial data base is being checked for the availability of permeability data (American Institute of Formation Evaluation 1989). Core analysis reports are also being reviewed. Once compiled, the permeability data will be "assigned" throughout the tight formations in a representative manner using appropriate statistical methods.

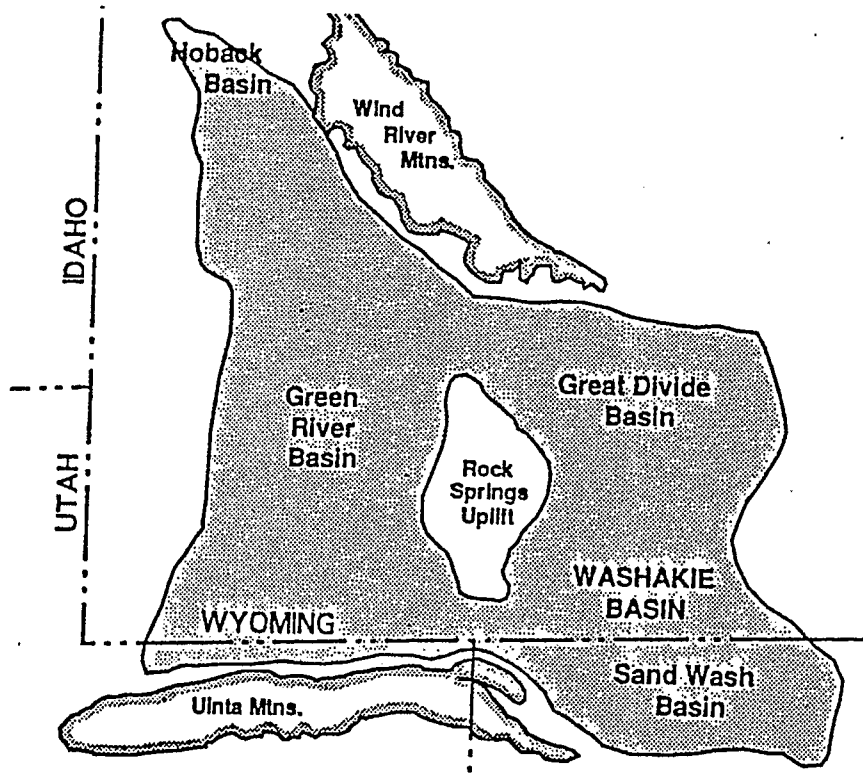


Figure 2. Washakie basin study area.
 (Greater Green River basin outlined by stippled area.)

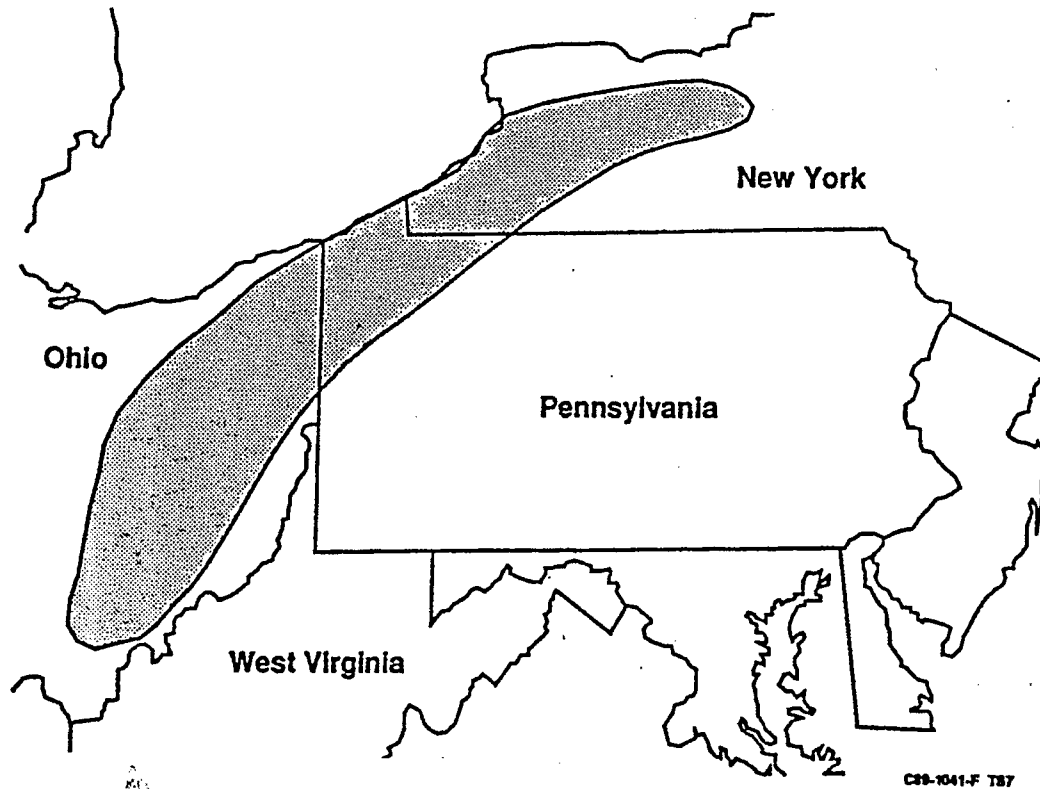


Figure 3. Location of the Clinton sandstone.

CS-1041-F 187

The capability to forecast gas production whenever improved technologies are implemented will be added to the systems model. Specifically, performance curves for horizontal wells producing from low permeability formations have been generated. Development of these performance curves was a separate support task for the systems analysis effort. The performance curves show that some reservoir situations are amenable to horizontal well completions. These reservoir situations are ones where induced fracture conductivity is limited or anisotropic permeability exists. Figure 4 shows a comparison of a typical vertically fractured well and horizontal wells, in terms of dimensionless cumulative production and dimensionless time. The inclusion of these forecasting curves will allow additional flexibility for estimating gas reserves as a function of technology.

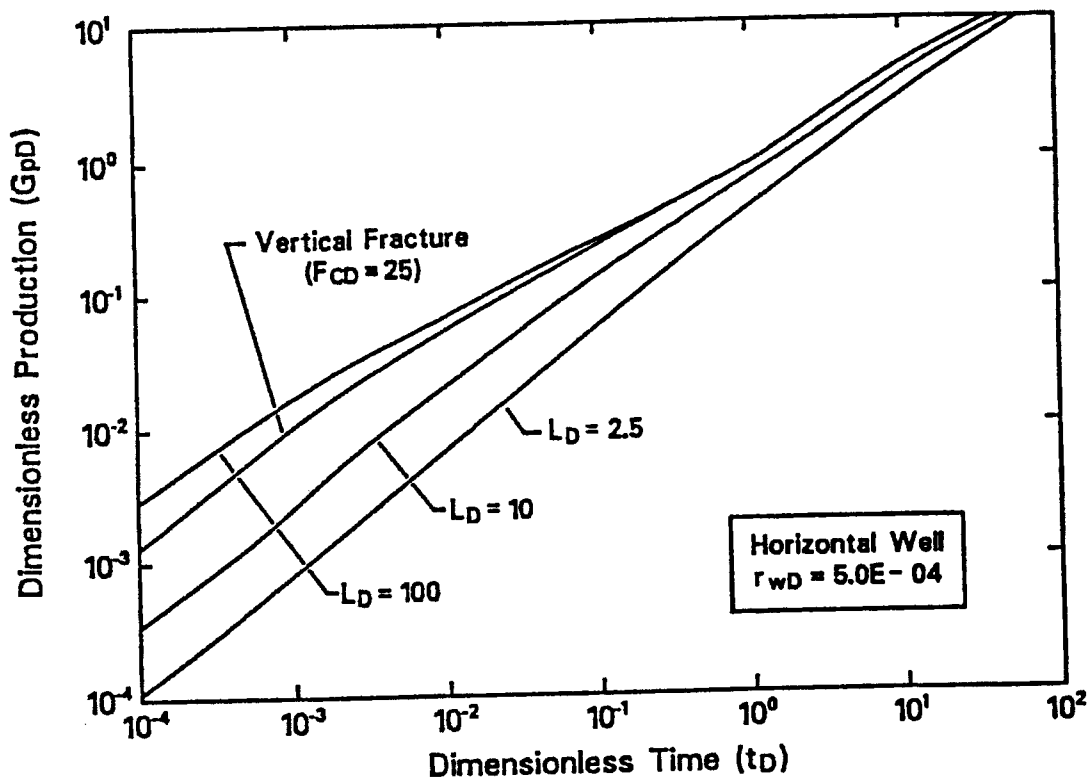


Figure 4. Horizontal well production type curves.

The systems model is structured to allow significant flexibility in the analysis of tight gas sands. Sensitivity analyses will be completed once reservoir descriptions and cost data are updated for the selected areas being appraised. These analyses will determine the influence of critical parameters including wellhead price, hydraulic fracture length, fracture conductivity, horizontal well recovery efficiency, etc. The new geologic interpretations will be included in the sensitivity analyses. Results of these analyses will indicate those factors which can significantly influence gas reserve increases from tight formations. The results are also expected to help guide future research efforts so that promising technologies can be brought closer to commercial application. Figure 5 shows typical results anticipated from the sensitivity analyses.

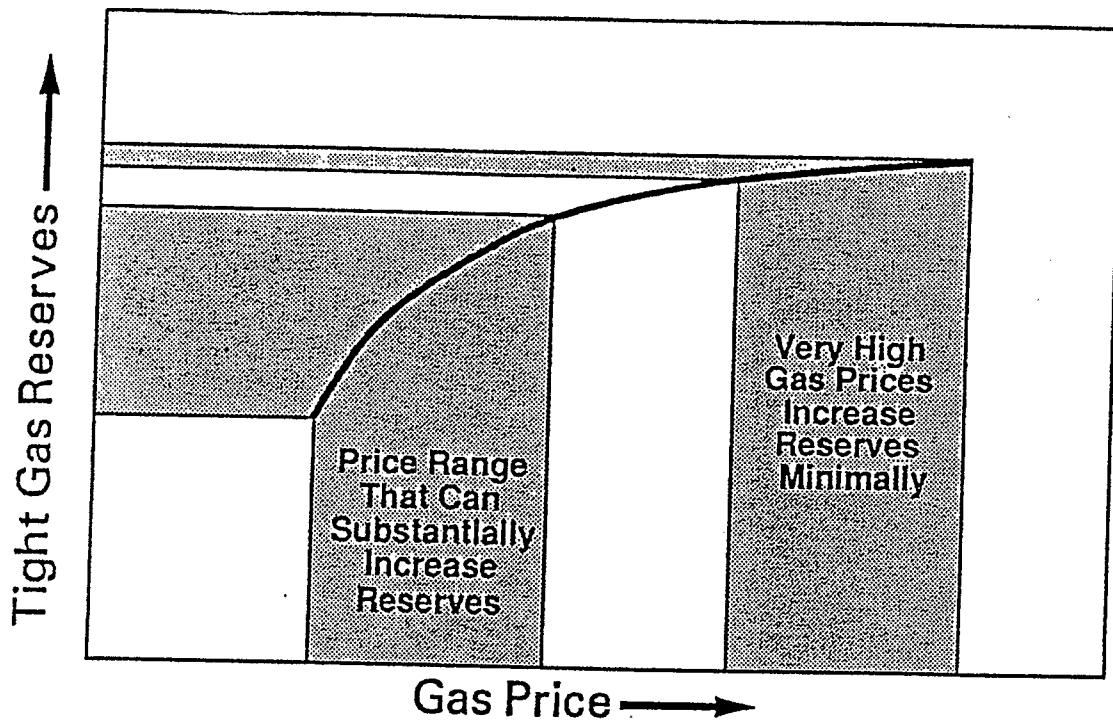


Figure 5. Typical sensitivity results, reserves versus gas price.

6. RESULTS/ACCOMPLISHMENTS:

Results to date can be generally grouped as "support tasks" for the systems modeling effort. Obtaining, compiling, and augmenting new geologic data for selected areas represent this type of support. The initial work has involved the Washakie basin in SW Wyoming and the Clinton formation in the eastern United States.

Cross-sections and other geological data are being used to define the vertical and areal extent of low permeability gas formations in these areas. Geophysical well logs and core analyses are being consulted to strengthen the characterizations. Analyses and compilation of these data for the Washakie basin are progressing on schedule; the task is scheduled for completion at the end of the 3rd quarter (fiscal year 89). Sensitivity analysis of the Washakie basin is scheduled for the 4th quarter of FY89.

Reservoir permeability data are required for technology assessment studies. A commercial data base of drill stem tests is presently being reviewed for permeability data availability/quality. Descriptions of the low permeability reservoirs underlying the Washakie basin will be augmented with these data leading to new estimates of recoverable gas.

A geologic description of the Clinton sandstone has been incorporated into the systems model although reservoir permeability values are still being compiled. Estimates of recoverable gas should be generated by year end, once the permeability data are secured and effectively distributed throughout the reservoir.

The project effort has led to the development of horizontal well production performance curves (type curves) for low permeability gas formations (Duda and Aminian 1989). These curves are based on a constant well flowing pressure and incorporate critical well and reservoir parameters such as vertical permeability, horizontal well length, and reservoir thickness. The curves were developed in terms of the real gas potential $[m(p)]$ using a finite-difference reservoir simulator. These type curves also provide a timely and cost effective means for initially forecasting the performance of horizontal wells. Currently, the performance curves are being structured for inclusion to the systems model so that the impact of horizontal well completions can be assessed.

7. FUTURE WORK:

Planned efforts call for continued resource appraisals of other priority basins/areas. These include the Uinta basin located in NE Utah and Devonian sandstones/siltstones located in the Appalachian basin. Updated geological characterizations will be used to estimate the volumes of recoverable gas.

Modifications of the systems model are also anticipated which will allow the assessment of new extraction technologies and geologic interpretations. One potential modification is the capability to forecast gas production using "novel" stimulation techniques. Other modifications concern implicit assumptions within the systems model. The timing of field development, once an area has been determined to be commercial, is one example.

Wellhead prices of natural gas are relatively low and fluctuate based on seasonal demands. These uncertainties, the supplies of conventional gas, and the use of alternative fuels will be considered in the development of new insights for tight gas resources. In addition, the availability of national and regional markets for low permeability gas will be included in the systems analysis.

8. REFERENCES:

American Institute of Formation Evaluation 1989. Data base of North American drill stem tests. 999 18th Street, Suite 1000, Denver, Colorado 80202.

Duda, J.R., and Aminian, K. 1989. Type Curves For Predicting Production Performance From Horizontal Wells in Low-Permeability Gas Reservoirs. SPE 18993 presented at the Joint Rocky Mountain Regional/Low Permeability Reservoirs Symposium, Denver, CO, March 6-8.

EG&G WASC, Inc. 1988. Memorandum to A. Zammerilli from H. Pratt, December 2.

Kuuskras, V.A., Brashears, J.P., Doshier, T.M., and Elkins, L.E. 1978. Enhanced Recovery of Unconventional Gas, The Program, Vol. II, U.S. Department of Energy, HCP/T2705-02. 537 p.

ICF-Lewin Energy 1988. TGAS-PC, Tight Gas Analysis System, User's Manual Version 2.01.

Law, B. E., et al. 1987. Geologic Characterization of Tight Gas Reservoirs, Annual Report FY1987, DE88010261. 50 p.
Morgantown Energy Technology Center 1987. Western Gas Sands Technology Status Report, DE87001030. 18 p.

National Petroleum Council 1980. Unconventional Gas Sources, Volume 5, Tight Gas Reservoirs, part 1. 222 p.

Spencer, C.W. 1985. Geologic Aspects of Tight Gas Reservoirs in the Rocky Mountain Region. Journal of Petroleum Technology, July Issue, pp 1308-14.

Supply-Technical Advisory Force 1978. National Gas Survey, Report to the Federal Energy Regulatory Commission on Nonconventional Natural Gas Resources: U.S. Department of Energy Federal Energy Regulatory Commission. 108 p.

Tyler, Theodore F. 1978. Preliminary chart showing electric log correlations of section A-A' of some Upper Cretaceous and Tertiary rocks, Washakie basin, Wyoming. USGS open file report 78-703.

United States Geological Survey/Minerals Management Service 1988. National Assessment of Undiscovered Conventional Oil and Gas Resources. Open file report 88-373, chapter 7.

GEOTECHNOLOGY OF LOW-PERMEABILITY GAS RESERVOIRS

2. CONTRACT NUMBER: DE-AC04-76DPO0789

CONTRACTOR: Sandia National Laboratories
 Geotechnology Research Division, 6253
 Albuquerque, NM 87185
 (505) 844 2302

CONTRACTOR PROJECT MANAGER: Dr. D. A. Northrop

PRINCIPAL INVESTIGATORS: Dr. N. R. Warpinski
 Dr. J. C. Lorenz
 Dr. A. R. Sattler

METC PROJECT MANAGER: K.-H. Frohne

PERIOD OF PERFORMANCE: April 1, 1988 to September 30, 1989

3. SCHEDULE/MILESTONES:

	A M J J A S O N D J F M A M J J A S
Piceance basin FE analyses	Δ _____
Viscoelastic analyses	Δ _____
Fracture origin studies	Δ _____
Study of archived core	Δ _____
Deformation/failure studies	Δ _____
Poroelastic measurements	Δ _____
Geostatistical fracture studies	Δ _____
Fracture property measurements	Δ _____
WGSS support activities	Δ _____

4. OBJECTIVES:

The objectives of this contract are to develop an understanding of the geotechnology associated with production of gas from tight, naturally-fractured, lenticular reservoirs of the western U.S. Specifically, this involves:

- characterizing the natural fracture system in western, tight, sandstone reservoirs;

- determining the relationship between the natural fractures and the in situ stresses and depositional environment;
- evaluating the interaction between stimulations and natural fracture systems;
- developing models of the origins of natural fracture systems found in the western basins; and
- analyzing unique and important rock/reservoir characteristics of these reservoirs.

5. BACKGROUND STATEMENT:

Exploration, stimulation and production of natural gas from low-permeability reservoirs of the western U.S. are dependent upon many of the geologic and geomechanical features of these reservoirs. The natural-fracture system is the critical feature in lenticular sandstone reservoirs of the Piceance basin, and probably in other western lenticular basins (Lorenz and Finley, 1989). Matrix rocks have microdarcy to submicrodarcy permeability, and since reservoirs are relatively small, production from such low-permeability matrix rocks is uneconomical under any foreseeable conditions. Natural fracture systems in these reservoirs are marginal, increasing the effective reservoir permeability to only a few tens of microdarcies, but this is sufficient for economic production, if wells can be completed and stimulated without damaging the natural fractures.

The natural fractures are narrow and easily susceptible to damage and plugging from water, drilling muds and stimulation fluids (Branagan et al., 1987, Sattler et al., 1988). A key finding of the Multiwell Experiment (Warpinski et al., 1988) was the demonstration of successful production from a lens in which special care was taken to avoid liquids damage during hydraulic fracturing. However, even under the best of circumstance, production is less than anticipated because hydraulic fractures parallel the primary natural fractures (Warpinski and Branagan, 1988). In these reservoirs, permeability anisotropies of 30:1 to 100:1 are deduced (Branagan et al., 1984 and Branagan et al., 1988) from three-well interference tests, with higher permeability in the direction of the primary natural-fracture set.

Successful production from these reservoirs will require a thorough understanding of the natural fractures, the relationship between the fracture system and the in situ stress field, and the damage mechanism in the natural fractures. Since reasonable production in such reservoirs is only likely in naturally-fractured lenses, a model for determining where fractures are likely to be found would be a powerful exploration tool. Thus the origin of the fracture system becomes an important element in the study of these reservoirs.

Our current studies address these particular features of these tight reservoirs, with emphasis on the origin and characterization of the

natural fracture system. Data from the Multiwell Experiment (MWX) site in the Piceance basin of western Colorado provide the focal point for analyses and experiments.

6. PROJECT DESCRIPTION:

The contract can be broadly divided into six categories, including:

- stress history;
- stress and fracture origins;
- deformation and fracture mechanics;
- geostatistical characterization of natural fractures;
- properties of natural fracture systems; and
- technical support to Western Gas Sands Subprogram (WGSS).

STRESS HISTORY

The stress history section can be divided into two main tasks: finite element calculations of the effect of the White River uplift and thrust, and viscoelastic calculations of the stress history of the Piceance basin, both near and away from MWX. We are conducting the finite element calculations to determine if the vertical distribution of natural fractures at MWX, as seen in Figure 1, are a result of the thrust fault. Figure 2 shows a schematic of how the thrust fault might increase or decrease the horizontal stresses at some point in the basin. Initial calculations show that the exact effect in the basin depends on many parameters, one of the more important being the coefficient of friction along the thrust plane.

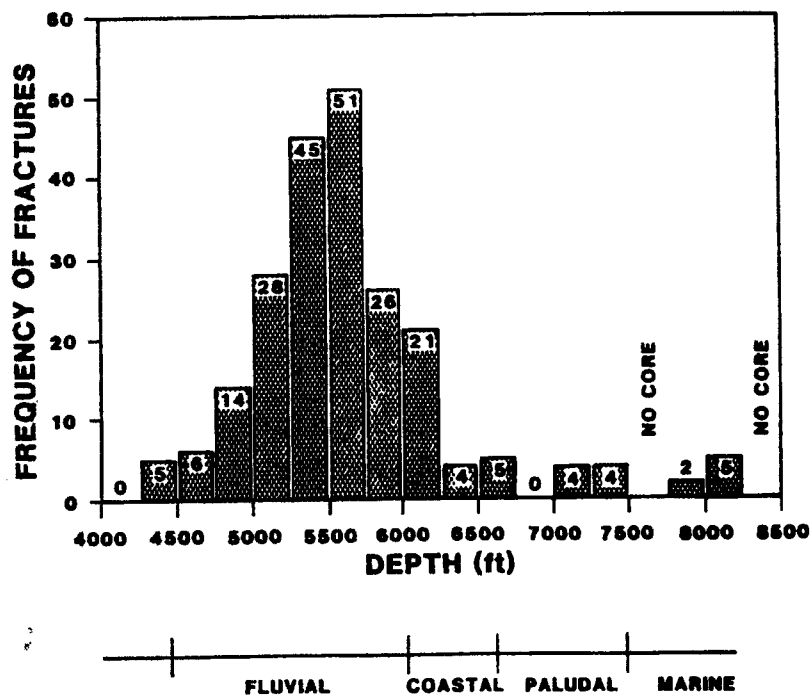


Figure 1. Histogram Of Extension Fractures

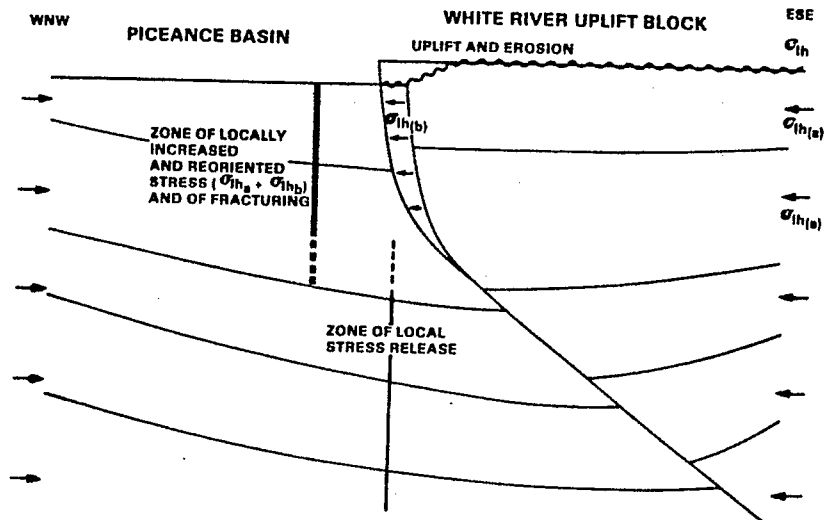


Figure 2. Effects Of Thrust

Viscoelastic calculations of the stress history of the basin are used to estimate the stresses at the time of fracturing. Previous analyses of the Cozzette Sandstone and Mancos Shale appear reasonable and set limits on viscoelastic parameters. Similar studies will be conducted for other intervals. Currently, we are modifying the computer code for general usage.

STRESS AND FRACTURE ORIGINS

This task deals specifically with the mechanism for fracture initiation and includes attempts to define the conditions under which fracturing occurred. Much of this work has been a gathering of information from the rock mechanics and geologic literature on regional fractures and failure mechanisms. Our purpose has been to find a plausible mechanism for the origin of regional fractures that is reconcilable with the fractures seen in core at MWX and those found in nearby outcrops in the Piceance basin. One of the key features of the fractures observed in MWX core is the nearly unidirectional orientation of the fractures, as seen in Figure 3.

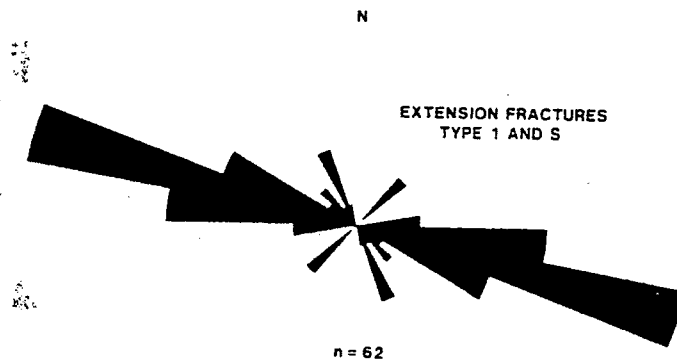


Figure 3. Fracture Strikes At MWX

We have found that the MWX fractures can be explained by simple extensional fracturing processes, even though the rocks were never in tension. Considerable rock mechanics data (e.g., Griggs and Handin, 1960) have shown that sedimentary rocks fail along the axis of compression when the net confining stress is relatively low. This process has been termed axial splitting, axial cleavage splitting and other terms, but we will simply refer to it as extensional fracturing. The fractures at MWX are believed to have formed at depth when pore pressure became very large, possibly approaching the overburden or lithostatic value. This effectively lowered the stress on the reservoir rocks, so that the net confining stress was minimal. Very importantly, however, there still was a differential horizontal stress due to tectonic forces and this differential stress, with the compressive component in the east-west direction, was sufficient to cause rock failure. As the tectonic stress increased slowly, or the pore pressure increased slowly, the effective load on the rocks increased, causing fractures to extend and dilate. A schematic of this process is shown in Figure 4.

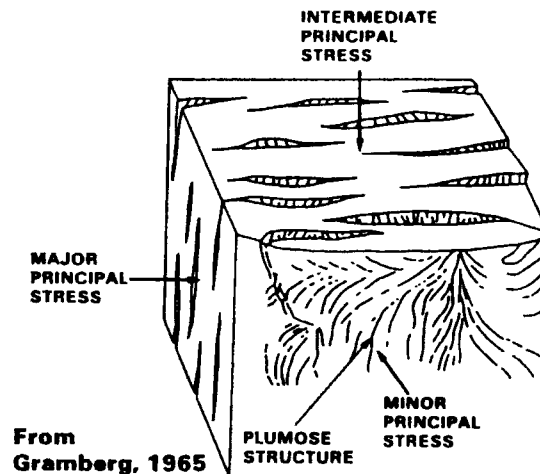


Figure 4. Schematic Of Extensional Fracturing

This mechanism is substantially different than natural hydraulic fracturing, although both rely on elevated pore pressures. Natural hydraulic fractures could be caused by elevation of pressure within the reservoir or injection from outside. Elevation of pressure within the reservoir is not likely since the stress in the reservoir will increase as the pore pressure increases, making it unlikely that oriented fracture sets could form. If the pressure is from some other layer and is injected catastrophically to cause large scale hydraulic fractures, then some rock residue should be found in the natural fractures, as in clastic dikes; no residue is seen in the MWX fractures. In addition, it is impossible to accommodate the large widths, the degree of mineralization, and the terminations at barriers with a natural hydraulic fracturing process.

Since an extensional fracturing process, such as the one that we propose, occurs very slowly, the strain associated with the fractures could have been easily accommodated by anelastic reorganization of the surrounding clay-rich rocks. Fractures could thus be held open for geologic time periods so that cement materials could be precipitated. The quasi-static nature of the process also accounts for the lack of fracture penetration into the bounding rock layers. It is also important to see that there is no mechanism for creating cross fracture sets, although structure, topography or other features could superpose other fracture sets.

This mechanism has been suggested previously (e.g., Gramberg, 1965), but the importance of pore pressure was not recognized then. We believe that this mechanism could have formed many of the regional fractures observed in flat-lying rocks in sedimentary basins. Currently, we are attempting to develop a more complete tectonic and stress history, to reformulate or revise crack stress models of this process, and to extrapolate this process throughout the Piceance and other western basins.

We are also obtaining and studying core from previous DOE cost-shared experiments in the Piceance basin to examine natural fractures, to estimate stress orientation relative to the fractures, to determine matrix permeability, and to compare well-test permeability with the matrix values. These results should help us determine how and where MWX results can be applied.

DEFORMATION AND FRACTURE MECHANICS

This task consists of two major parts. The first part is to measure deformation and failure characteristics of MWX rocks under low confining stresses, in the presence of water, at very low strain rates (to simulate geologic conditions), and possibly at elevated temperatures. The purpose is to obtain needed failure data to evaluate our extensional fracturing hypothesis. The second part consists of obtaining poroelastic properties of the MWX reservoir rocks and determining usable effective stress laws for important processes, such as permeability and deformation. An old permeability apparatus has been reconditioned to provide some of this information; load frames and pressure/temperature vessels are already available for other tests. A very important part of this testing will be a study of ways to minimize the effects of relaxation microcracks on these measurements.

GEOSTATISTICAL CHARACTERIZATION OF NATURAL FRACTURES

This category consists of devising a methodology for characterizing the fractures seen at MWX and in the outcrop for use in models and geologic analyses. We have completed the examination of over 2000 natural fractures found in the 4100 ft of MWX core and published the results (Finley and Lorenz, 1988 and 1989). One of our next tasks is to reanalyze the MWX fractures in terms of bed thickness, depositional environment, depth, location in the frequency spectrum, etc. to estimate spacing and other important fracture parameters. We have already developed the methodology for this reanalysis, and we will soon begin

obtaining the necessary data. From outcrop, we have accumulated some information on the angular, length and interconnection distributions of the natural fractures.

PROPERTIES OF NATURAL FRACTURE SYSTEMS

The purpose of this study is to obtain additional information on the flow properties of the natural fracture system. Effects of water saturation and stress are important considerations. We also will attempt to evaluate the contribution, if any, of the low angle shear fractures (seen in many mudstone or carbonaceous stringers within the reservoirs) to the effective reservoir permeability. If there is any significant permeability associated with these fractures, then a mechanism is available for enhanced permeability in directions normal to the principal fracture azimuth.

TECHNICAL SUPPORT TO WGSS

The purpose of this task is to provide technical support to the Western Gas Sands Subprogram in areas of sedimentology, natural fractures, geomechanics, in situ stress, stimulation, and laboratory studies. One such area is a review of MWX data to look at production as a function of stress ratios, effective stress ratios, overpressuring ratios, stress contrast ratios, and any other functions that might provide an enhanced rationale for predicting where and explaining why production may be favorable in a given locale. Some of these results are interesting, but equivocal. For example, Figure 5 shows the initial gas production per unit lens thickness versus the effective stress ratio (horizontal divided by the overburden) of the reservoirs. While there is clearly a relation between production and the effective stress ratio, the data are grouped by depositional environment as well. It is impossible to separate out the effects of the stress ratio compared to the depositional environment. Additionally, the effective stress ratio variation is due almost entirely to pore pressure and a plot of production versus pore-pressure ratio would look similar to Figure 5. This implies that improved gas production can be correlated with overpressuring, which is fairly obvious, since higher pore pressures result in a higher pressure difference and a greater fracture conductivity (less normal stress across the fracture).

Other areas of support include continuing to maintain and update important MWX databases, finish papers and reports associated with MWX, and provide information for the upcoming slant-hole project at the MWX site.

7. RESULTS AND ACCOMPLISHMENTS:

- We have developed a mechanism for the origin of the natural fractures found at depth at the MWX site. This mechanism is consistent with the features found in core, the estimated stress and pore-pressure history, and mechanics principals and laboratory data.

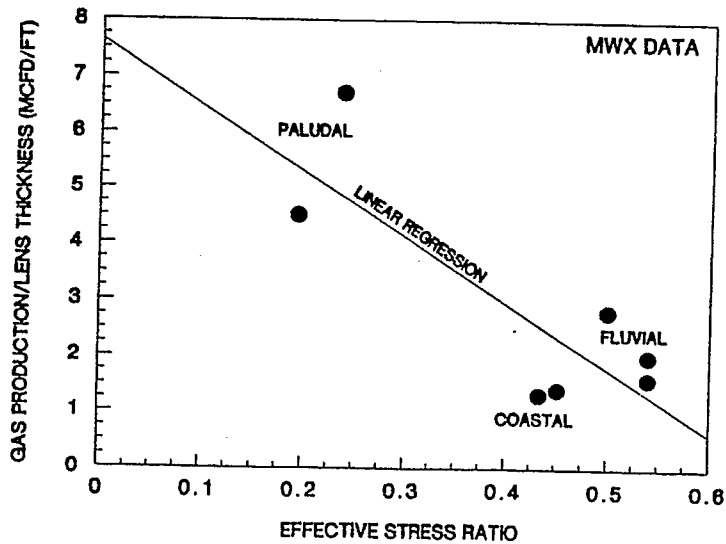


Figure 5. Production Versus Effective Stress Ratio

- We have completed the analysis of over 2000 natural fractures found in MWX core and developed preliminary interpretations.
- We have correlated the tectonic history with origins of the natural fractures. Good agreement is found for timing and orientation of the fractures. Finite element and viscoelastic models show good agreement with this history.
- We have completed the redeployment of the permeability lab for poroelastic studies. Initial studies are being conducted.
- We have completed a correlative study of reservoir and rock properties as a function of depositional environment, as well as lithology (Lorenz et al., 1989)
- We have analyzed MWX results in terms of stress ratios, effective stress ratios, overpressure ratios, horizontal stress differences, and other parameters that may control fracture production. However, the depositional environment appears to be the overriding factor.
- We have conducted studies of archived MWX core which show that old sandstone cores can be accurately reanalyzed for permeability. Archived cores from previous DOE experiments have been located.

8. FUTURE WORK:

Future plans include additional analyses of the MWX fractures, revision of tectonic histories as new data become available, finite element analyses of the stress state and failure mode, poroelastic and reservoir property studies, measurement of deformation and failure characteristics for these rocks, and geostatistical analyses of fracture distributions.

9. REFERENCES:

- Branagan, P.T., Cotner, G. and Lee, S.J. 1984. Interference Testing of the Naturally Fractured Cozzette Sandstone: A Case Study at the DOE MWX Site. SPE 12869. Proceedings, SPE/DOE/GRI Unconventional Gas Recovery Symposium:359-366. Pittsburgh, PA.
- Branagan, P.T., Cipolla, C.L., Lee, S.J. and Yan, L. 1987. Case History of Hydraulic Fracture Performance in the Naturally Fractured Paludal Zone: The Transitory Effects of Damage. SPE 16397. Proceedings, 1987 SPE/DOE Joint Symposium on Low Permeability Reservoirs:61-72. Denver, CO.
- Branagan, P.T., Lee, S.J., Cipolla, C.L. and Wilmer, R.H. 1988. Pre-Frac Interference Testing of a Naturally Fractured, Tight Fluvial Reservoir. SPE 17724. Proceedings, 1988 Gas Technology Symposium:193-208. Dallas, TX.
- Finley, S.J. and Lorenz, J.C. 1988. Characterization of Natural Fractures in Mesaverde Core from the Multiwell Experiment. Sandia Natl. Labs. Report SAND88-1800.
- Finley, S.J. and Lorenz, J.C. 1989. Characterization and Significance of Natural Fractures in Mesaverde Reservoirs at the Multiwell Experiment Site. SPE 19007. Proceedings, 1989 Joint Rocky Mountain Regional/ Low Permeability Reservoirs Symposium:721-728 Denver, CO.
- Gramberg, J. 1965. Axial Cleavage Fracturing, a Significant Process in Mining and Geology. Engineering Geology: 1:31-72.
- Griggs, D. and Handin, J. 1960. Observations on Fracture and a Hypothesis of Earthquakes. Geological Society of America Memoir 79:347-364.
- Lorenz, J.C. and Finley, S.J. 1989. Differences in Fracture Characteristics and Related Production: Mesaverde Formation, Northwestern Colorado. SPE Formation Evaluation 4(1):11-16.
- Lorenz, J.C., Sattler, A.R. and Stein, C.L. 1989. Differences in Reservoir Characteristics of Marine and Nonmarine Sandstones of the Mesaverde Group, Northwestern Colorado. Sandia Natl. Labs Report, SAND88-1963.
- Sattler, A.R., Raible, C.J., Gall, B.L. and Gill, P.J. 1988. Stimulation-Fluid Systems for Naturally Fractured Tight Gas Sandstones: A General Case Study from Multiwell Experiment Stimulations. SPE 17717. Proceedings, SPE Gas Technology Symposium:117-130. Dallas, TX.
- Warpinski, N.R. and Branagan, P.T. 1988. Altered-Stress Fracturing. SPE 17533. Proceedings, SPE Rocky Mountain Regional Meeting:465-476 Caspar, WY.

Warpinski, N.R., Branagan, P.T., Sattler, A.R., Cipolla, C.L., Lorenz, J.C. and Thorne, B.J. 1988. A Case Study of a Stimulation Experiment in a Fluvial, Tight, Sandstone Gas Reservoir. SPE 18258. Proceedings, 63rd Annual Technical Conference and Exhibition of the Society of Petroleum Engineers:751-764. Houston, TX.

**ROCK MATRIX AND FRACTURE ANALYSIS OF FLOW
IN WESTERN TIGHT GAS SANDS**

1. CONTRACT NUMBER: DE-AC21-84MC21179

CONTRACTOR: New Mexico Petroleum Recovery Research Center
New Mexico Institute of Mining and Technology
Socorro, NM 87801
(505) 835-5403

CONTRACTOR PROGRAM MANAGER: F.D. Martin

PRINCIPAL INVESTIGATOR: Norman R. Morrow

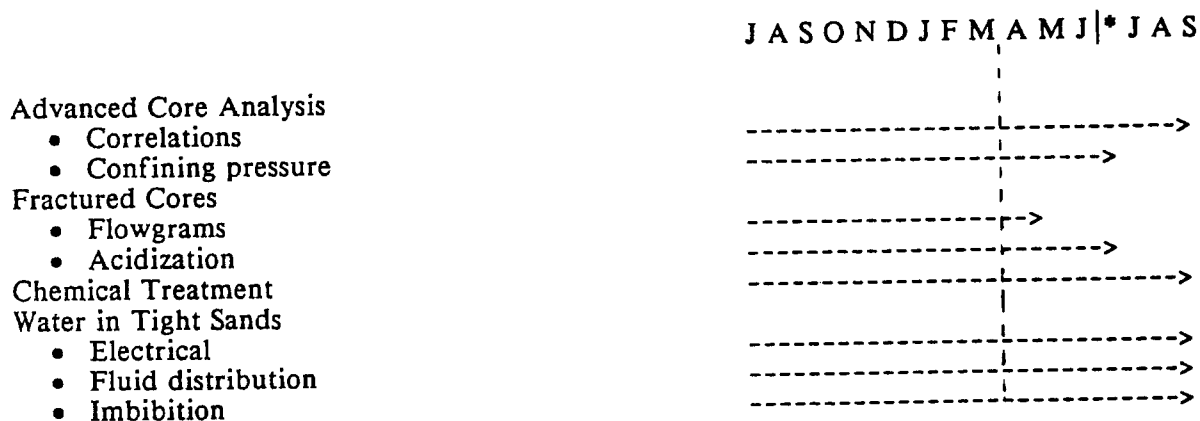
PROJECT CONTRIBUTORS: J.S. Buckley Shouxiang Ma
M. Cather M.L. Graham
K.R. Brower B. Gonzales
Xiaoyun Zhang

METC PROJECT MANAGER: Karl-Heinz Frohne

CONTRACT PERIOD OF PERFORMANCE: June 1984 - April 1989

2. SCHEDULE/MILESTONES:

1988-89 Program Schedule



*No cost extension on State of New Mexico supported part of project.

3. OBJECTIVES:

The investigation concerns the relationship of pore structure to transport properties of tight gas sands and has four main objectives:

- To determine properties of the rock matrix by advanced core analysis procedures.
- To determine the effect of natural fractures on gas flow.
- To measure changes in rock properties caused by chemical treatment.
- To determine the effect of water saturation on gas flow and electrical properties of low permeability sands.

4. BACKGROUND STATEMENT:

The Western Tight Gas sands, potentially a major source of natural gas, have been studied

for several years. These sands are characterized by very low porosity and permeability. The main problem in developing the resource is that of efficiently extracting gas from the reservoir. Future production depends on a combination of gas price and technological advances. Gas production can be enhanced by stimulating the reservoir through fracturing. Studies have shown that many aspects of fracture design and gas production are influenced by properties of the rock matrix. Also, recent research has indicated that the flow conditions in the reservoir can be greatly enhanced by the presence of natural fractures, which serve as a transport mechanism for gas from the less permeable rock portions. Computer models for stimulation procedures require accurate knowledge of flow properties of both the rock matrix and the fractured regions. These advanced core analysis procedures are aimed at understanding the relationship between pore structure and these properties.

The Multiwell project provides a unique opportunity to measure the properties of cores taken from zones for which numerous other geologic, laboratory, and field investigations have been performed. The investigation is funded jointly by the U.S. Department of Energy and the State of New Mexico.

5. PROJECT DESCRIPTION:

ADVANCED CORE ANALYSIS

- Comparison of porosity measurement by thin section to volumetric measurement.
- Measurement of permeability vs. overburden pressure relationships.
- Determination of water adsorption and desorption isotherms.
- Measurement of surface area by either nitrogen adsorption or H_2-D_2 exchange, or both.
- X-ray analysis to identify clay types that may adversely affect stimulation treatments and production.
- Determination of effects of overburden pressure on permeability to water and relative permeability; investigation of electrical resistivity vs. saturation relationship.
- Mineral analysis of thin section.
- Examination of pore structure through pore casts.

INVESTIGATION OF THE EFFECT OF NATURAL FRACTURE SYSTEMS ON GAS FLOW

- Investigation of flow along and across selected samples as a function of overburden pressure.
- Measurement of the effect of water content on permeabilities of cores containing fractures.
- Measurement of the effects of acid treatment on mineralized fractures and the study of possible formation damage to the surrounding rock matrix.

INVESTIGATION OF PORE-FILLING MATERIALS AND CEMENTS IN LOW-PERMEABILITY SANDSTONES BY CHEMICAL METHODS

- Investigation of the role of cements and pore-filling materials in controlling gas flow by selective dissolution.
- Examination of possibilities of permeability enhancement (stimulation) by chemical methods.

EFFECT OF WATER ON GAS PRODUCTION

- Determination of the effect of water saturation on gas permeability at various levels of confining pressure.
- Complementary measurements of electrical properties as a function of water saturation and overburden pressure.

- Measurements of capillary pressure relationships by high speed centrifuge and extension of capillary pressure results to above 1000 psi by desorption isotherms.
- Relation of gas flow behavior to the microscopic distribution of water within the pore spaces.
- Determination of effect of drying on pore structure.

6. RESULTS/ACCOMPLISHMENTS:

- A technique for estimating pore quality from thin sections has been developed.
- Pressure sensitivity of low permeability MWX sandstones has been shown to correlate with diagenetic facies.
- Detailed petrographic analyses, including mineralogy, diagenetic history, and pore quality, structure, and distribution have been completed for thirty MWX samples.
- Absolute and relative permeabilities have been measured for cores containing natural calcite-filled fractures at various overburden pressures. Acetic acid treatment greatly enhances permeability of samples containing calcite-filled fractures.
- Absolute and relative permeabilities have also been measured for core plugs containing calcite-filled fractures before and after refracturing along the preexisting plane of weakness.
- Preserved (undried) cores have been tested and then subjected to drying to determine the effects of drying on permeability to brine.
- Various chemical treatments have been applied to cores to determine which minerals occupy pore space and hence control permeability.
- Capillary pressure measurements made by high speed centrifuge have been found to be in reasonable agreement with mercury injection measurements at intermediate pressures.
- Formation factors give linear log-log relationships with gas and brine permeabilities at varied overburden pressures.

Results and discussion related to the above accomplishments have been reported. These are summarized as follows:

Advanced core analysis for all Multiwell cores on hand is complete. Measurements have included Klinkenberg permeabilities for first unloading at overburden pressures of 500 and 5000 psi, surface areas (BET), porosity determination, and crack thickness estimates. For selected samples, additional methods of detailed core analysis have included measurements of capillary pressures by various methods, detailed petrographic analysis for lithology and porosity information, formation factor evaluation at various overburden pressures, and clay mineral analysis by X-ray diffraction.

Preliminary studies on the effect of chemical treatment on flow properties of rock matrix are now complete. Current work is concentrating on the use of NaOH and HCl as reagents to determine if results seen in the preliminary studies are consistent for a given depositional environment or general lithology. By noting changes in flow properties for various treatments, and comparing these with changes visible in thin section or by SEM, it may be possible to determine which mineral constituents of the rock matrix are important in controlling fluid flow behavior in tight gas sands.

Changes in formation factors of low permeability gas sands with changes in overburden pressure have been compared using both gas and brine as fluids. Linear relationships were found in log-log plots of brine and gas permeability vs. formation factor, though slopes for the lines are somewhat different, indicating different pressure sensitivity behavior. Capillary pressures measured by high speed centrifuge have been compared with those obtained for duplicate core plugs measured using mercury injection. Curves are similar in shape and value at low and intermediate capillary pressures.

In this report we focus on work concerned with flow in healed tectonic fractures.

FLUID FLOW IN VERTICAL MINERALIZED FRACTURES (VMF)

Gas production from the Mesaverde Group measured during the course of the Multiwell Experiment was often one to three orders of magnitude greater than predicted from measurements of matrix permeabilities. It was concluded that natural fractures contribute significantly to observed production (Lorenz et al 1986). Many of the fractures in sandstone intervals are readily identifiable because of mineralization which, in most cases, appears to fill the fracture space. However, the rock matrix is generally of only a few microdarcies permeability, and it is not obvious whether the mineralized fractures serve as a conduit or a barrier to gas flow.

In this report we summarize work on the following topics:

- Flow properties of core plugs containing vertical mineralized fractures (VMF's) relative to the neighboring matrix.
- Relative permeability behavior of VMF cores.
- Permeability enhancement through refracturing and acidization of mineralized fractures.

Permeability Measurements

Confining stress used to simulate overburden pressure is applied by 3-D hydrostatic loading on cylindrical cores. In preparing matrix and fractured plugs, cores were cut in several directions and positions relative to the fracture. Orientations of matrix samples and samples containing VMF's are indicated in Fig. 1.

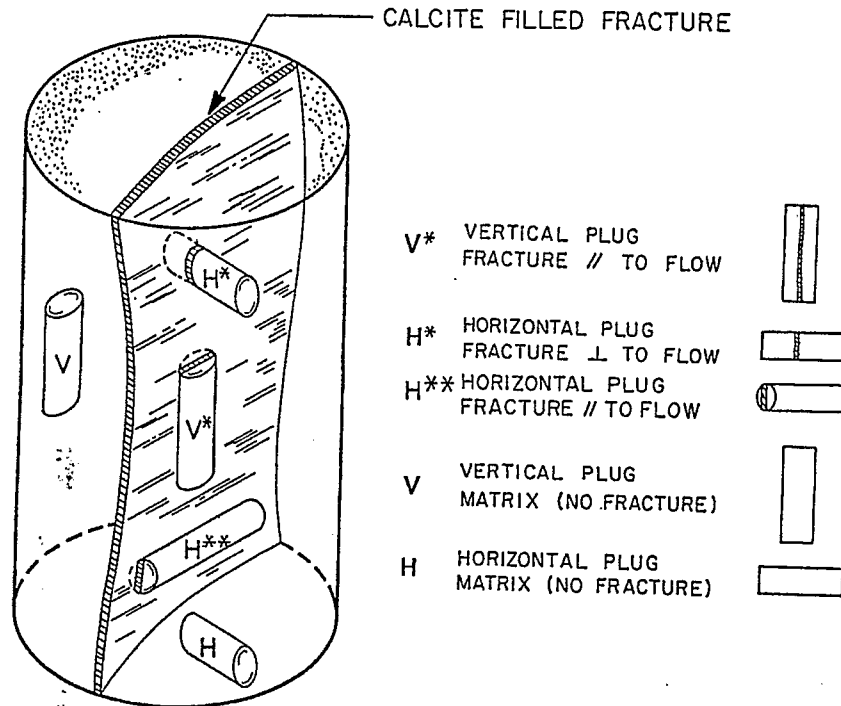


Figure 1. Orientation of Plugs from Whole Core Sample

The apparatus used for permeability measurements and the general procedure have been described previously (Brower & Morrow, 1985). Behavior under stress of cores containing fractures was broadly comparable to the matrix behavior although examples of extreme pressure sensitivity were sometimes encountered. In the present investigation, we adopted a range of nominal confining pressure, P_{cf} , of 500 psi to 5,000 psi. Example results for first loading, first unloading, second loading, and second unloading are shown in Fig. 2. Although there is always some hysteresis between loading and unloading, reproducibility of the hysteresis loop and reproducibility of the k_{5000} results obtained after first and second loading indicated that permanent damage to the core from stress cycling was fairly minimal.

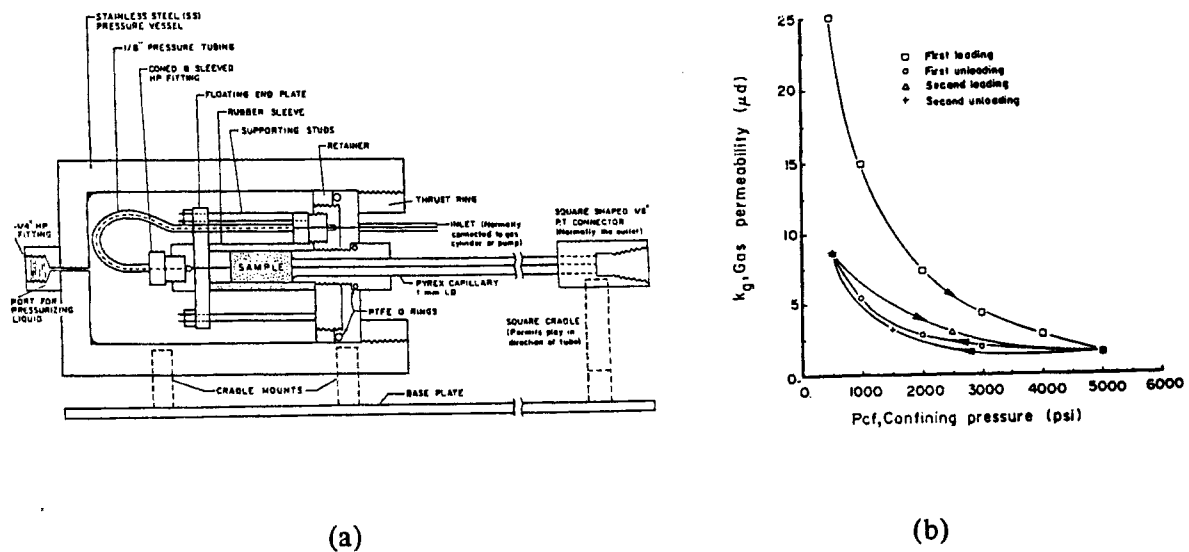


Figure 2. (a) Permeability Apparatus, and (b) Typical Relationships between Gas Permeability and Confining Pressure.

The first loading curve is commonly used to characterize pressure sensitivity. However, these results include long-term stress relaxation effects which are not readily reproduced (Kilmer, Morrow & Pitman, 1987). Results for first and second loading were obtained in preliminary work. Once the advantages of preloading the core became clear, measurements were standardized on the change in permeability for first unloading from 5,000 psi to 500 psi. Two distinct advantages of not using first loading results are 1) that long-term strain relaxation effects are avoided and, 2) application of high pressure gives adequate sealing between the Hassler sleeve and the core even when the confining pressure is decreased to far below the 800 - 1,000 psi lower limit that is sometimes adopted for tight gas sands (Jones & Owens, 1981). Linearity of $\log k_g$ vs. $\log P_{cf}$ relationships for all matrix and fractured samples was tested for up to ten data points over the range 500 psi to 5,000 psi using a constant differential pressure for gas flow. Klinkenberg plots were prepared for end point confining pressures of 500 and 5,000 psi and sometimes at an intermediate value of 2,000 psi. A pressure sensitivity ratio (PSR) was defined by $k_{\infty,500}/k_{\infty,5000}$ where the numbers in the subscripts indicate P_{cf} .

Results of comparisons between matrix and VMF plug permeabilities are presented in Tables 1 and 2, and in Fig. 3. Plots of k_{vm} vs. k_v for both high and low confining pressure

show k_{v*} to be generally higher than or close to k_v (Fig. 4). However, there is only one instance of k_{v*} exceeding k_v by more than an order of magnitude, and, in this case (MWX-1 29-7B V*), the plug contained two fractures. For the majority of samples, k_{v*} is about double k_v . Values of k_{H*} and k_H are generally scattered about the 45° line in Fig. 4 showing that the fractures do not enhance permeability or serve as a barrier to crossflow under the conditions of measurement. An unexpected feature of the results is that the PSR of the VMF and matrix samples are in close agreement (see Fig. 5).

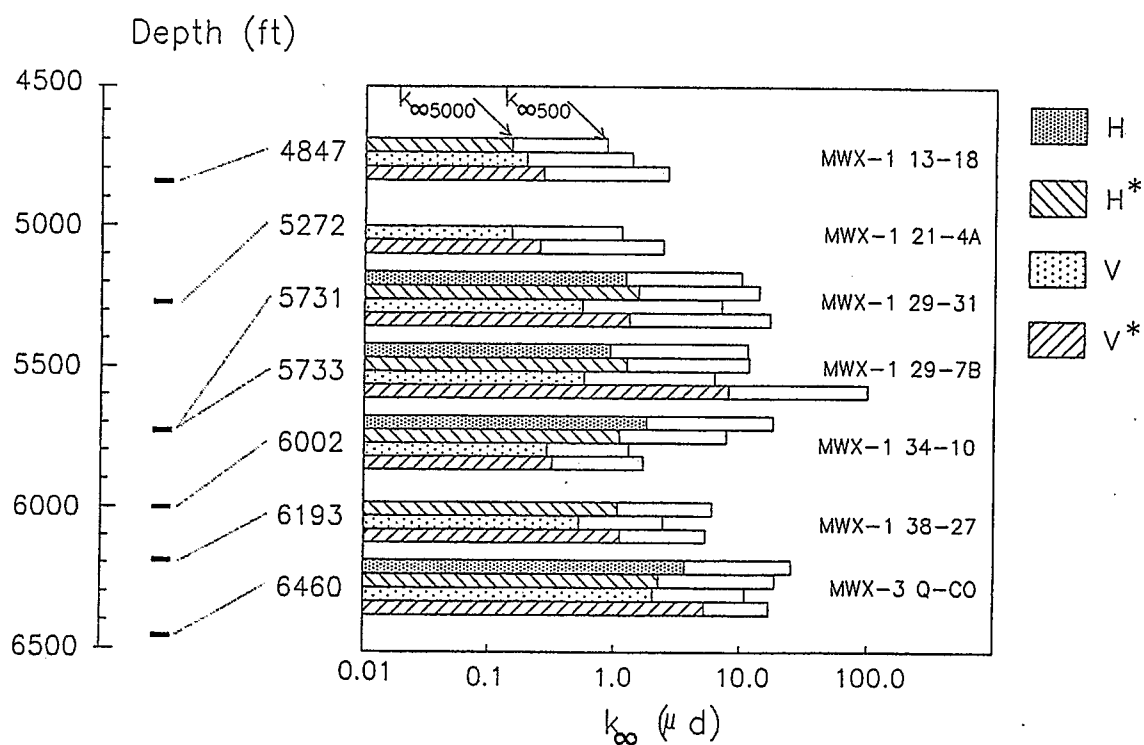


Figure 3. Summary of MWX Matrix and VMF Permeability Behavior (first unloading or second loading).

Table 1. Properties of HVF and Matrix Core Samples Given by First and Second Loading

Core Sample	Orientation	Porosity (%)	Surface Area (m ² /g)	First Loading			Second Loading		
				K _{w500} (μd)	K _{w5000} (μd)	$\frac{K_{w500}}{K_{w5000}}$	K _{w500} (μd)	K _{w5000} (μd)	$\frac{K_{w500}}{K_{w5000}}$
MWX-1 13-18 4846.5- 4847 ft.	V*	4.06	0.89	5	0.235	21.28	2.6	0.265	9.81
	V	4.63	0.96	2.3	0.2	11.5	1.35	0.195	6.92
	H*	4.41	1.5	8.8	0.17	51.7	0.85	0.15	5.67
MWX-1 21-4A 5271.6- 5272 ft.	V*	3.69	0.92	11.5			2.4	0.25	9.6
	V	4.7	1.15	1.1	0.12	9.17	1.13	0.1	7.53
MWX-1 29-31 5730.9- 5731.2 ft.	V*-I	7.01	1.14	36	1.3	27.69	17	1.05	16.19
	V	7.1	1.21	15.5	0.55	28.18	7	0.45	15.56
	H*	7.14	1.11	20.1	1.3	15.46	12.8	1.12	11.43
	H	7.02	1.07	18.5	1.35	13.7	10	1.1	9.09
MWX-1 34-10 6002.3- 6002.5 ft.	V*	4.57		4.3	0.32	13.44	1.7	0.32	5.31
	V	4.5		4.4	0.24	18.33	1.3	0.29	4.48
	H*	4.52		21	1.2	17.5	7.6	1.1	6.9
	H	4.97		60	2	30	18	1.8	10

Table 2. Properties of VMF and Matrix Core Samples Given by First Unloading

Core Sample	Orientation	Porosity (%)	Surface Area (m ² /g)	First Unloading		
				k _{w500} (μd)	k _{w5000} (μd)	$\frac{k_{w500}}{k_{w5000}}$
MWX-1 29-31 5730.9- 5731.2 ft.	V*‡	7.01	1.14	17	1.3	13.1
	V	7.10		7	0.55	12.7
	H*	7.30		13.9	1.54	9
	H	7.02		10	1.22	8.2
MWX-1 29-7B 5733.2- 5733.6 ft. (double fracture)	V*	6.23		100	7.98	12.5
	V	6.88		6.19	0.57	10.9
	H*	7.06		11.6	1.25	9.3
	H	7.11		11.3	0.91	12.4
MWX-1 38-27 6192.6- 6193 ft.	V*	6.02		5.23	1.12	4.7
	V	5.98		2.43	0.53	4.6
	H*	6.11		5.94	1.07	5.6
MWX-3 Q-CO 6459.2- 6460 ft.	V*	8.39	2.7	16.9	5.2	3.25
	V	8.89	3	10.9	2.05	5.32
	H*	8.47	2.97	18.58	2.38	7.81
	H**	7.13		19.75	7.96	2.48
	H	8.81	3.16	25.16	3.64	6.91

‡Duplicate sample with respect to MWX-1 29-31 of Table 1.

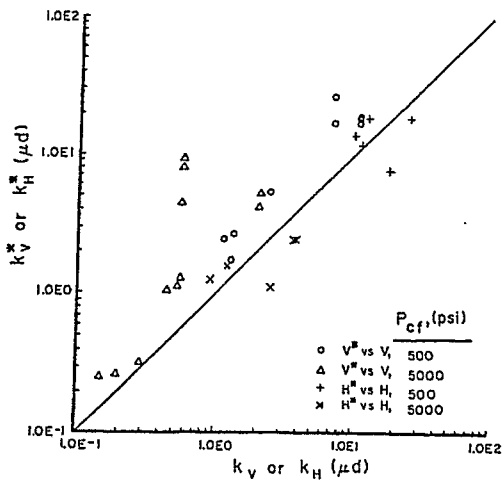


Figure 4. VMF Permeability vs. Matrix Permeability for Plugs Cut in V*, H*, V, and H Orientations (see Fig. 2).

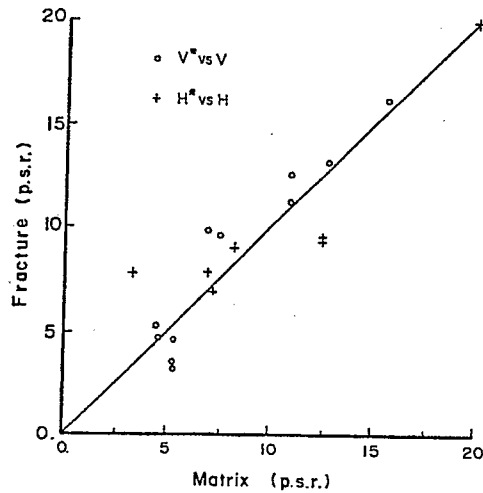


Figure 5. Pressure Sensitivity Ratio ($k_{\infty,500}/k_{\infty,5000}$) of VMF Cores vs. Matrix.

The pressure sensitivity exhibited by the fracture provides a strong indication that fracture permeability is controlled by sheet pores at grain boundaries (Brower & Morrow, 1985) that respond to change in stress in a manner comparable to sheet pores in the matrix. This conclusion is supported by reflected fluorescent light images of pore space given by surface-stained thin sections.

Relative Permeabilities

For measurement of relative permeabilities to gas at different levels of water saturation, the desired levels of water saturation were achieved by controlled evaporation with measurements being made at nominal saturations, S_w , of 60%, 45%, 30%, and 15% water. Absolute permeability to gas was measured after oven-drying the core at 110°C.

Relative permeability measurements were made for gas flow in matrix samples and for flow along and across VMF's. Results for each core are plotted as k_{rg} vs. S_w with a confining pressure as a parameter and as k_g vs. P_{cf} with S_w as parameter (Figs. 6 and 7). Results obtained for matrix samples have been reported previously. For plug MWX-1 29-7B H* (cut so that flow was across the fracture), Klinkenberg plots were made at three levels of confining pressure and five levels of water saturation (Fig. 6). This plug contained two parallel healed fractures of about 1mm in width spaced about 3mm apart. Relative permeability results for flow across the fracture were qualitatively similar to typical matrix results.

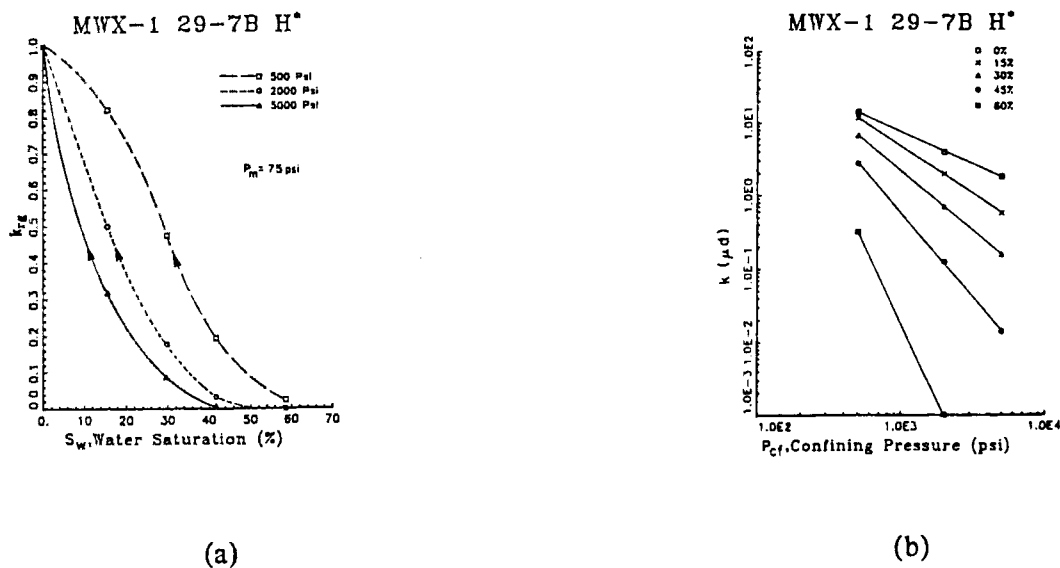


Figure 6. Relative Permeability Behavior for a Plug With H* Orientation.

Results for gas relative permeabilities for flow along the fracture for a core having orientation V* are shown in Fig. 7. Relative permeabilities were distinctly higher than for matrix material or for flow across the fracture, especially at high water saturations. Two other fractured cores were tested and gave the same behavior.

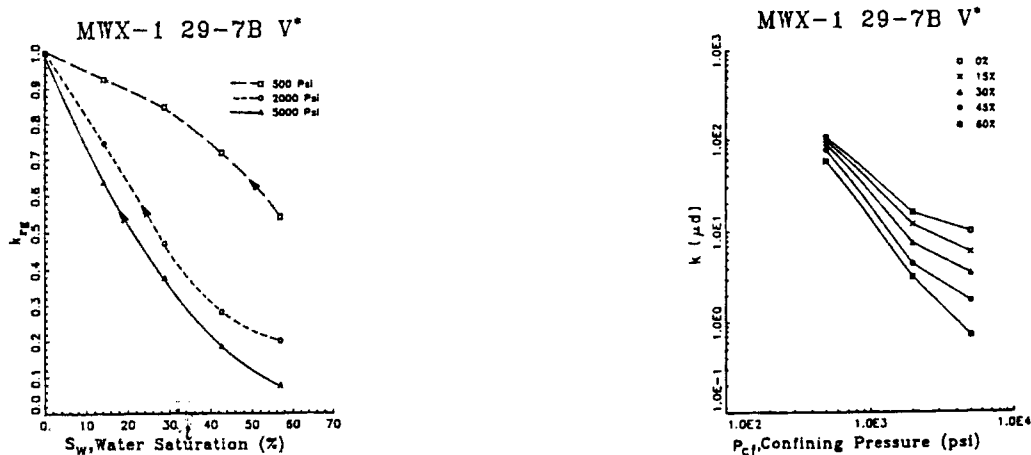


Figure 7. Relative Permeability for Flow Along Fractures (V* orientation).

The results show that the mineralized fractures were much more conductive than the neighboring matrix, particularly at high water saturation and low confining pressure. Thus, the contribution to gas flow of the fracture relative to the matrix is greatly enhanced by the presence of water. This conclusion supports the argument (Lorenz et al, 1986) that hydraulic

fracturing could result in temporarily decreased gas production if the fracture system becomes loaded with liquid.

Flowgrams

Comparison of flow in cores containing mineralized fractures with neighboring matrix core provides an indication of the contribution of the fracture to flow. In order to test fracture permeability directly, a technique was devised using elementary principles of photography for indication of gas velocities in the fracture relative to the immediate matrix. The fractured core plug selected for testing was mounted into a piece of vacuum hose that served as a Hassler sleeve with an AgCl impregnated paper disc backed by a small piece of Berea sandstone on the outflow side of the plug. An appropriate volume of H₂S was swept through the sample by nitrogen at 350 psi. The density of disc coloration from deposition of silver sulfide showed whether the fracture was more or less conductive than the neighboring matrix.

Flowgrams confirmed, in all cases except one, that the mineralized fractures were more conductive than the neighboring matrix. The image produced by the fracture suggested that fracture conductivity resulted from the mineralized region as a whole having some characteristic permeability rather than being from one or two fine cracks of distinctly less complete mineralization.

Acetic Acid Treatment

It has been shown that calcite-filled fractures are usually more conductive than the matrix, but that permeabilities are still low, usually being of the same order as the surrounding matrix. The high concentration of calcite within these fractures offers the possibility that fracture conductivity could be enhanced by acidization. A second significant observation with respect to formation stimulation is that the calcite-filled fractures provide planes of weakness. In the formation penetrated by the MWX wells, the VMF's are strongly oriented in a direction perpendicular to the present direction of least principal stress (Finley & Lorenz, 1989). Thus, if the reservoir is fractured artificially, refracturing of the formation may tend to part along the mineralized planes. If acid or acid-foam fracturing is employed, the combined irregularity of the fractures and chemical removal of calcite may lead to highly conductive fractures which may even be self-propping. If there is no need to carry a propping agent and if leak-off into the tight sand matrix can be kept low (Warpinski, 1989), fracture fluid design would be greatly simplified.

A possible advantage of stimulating calcite-filled fractures as opposed to carbonate formations is that the width of the etched fracture will not exceed the width of the calcite filling. Thus, unlike acidization of carbonates (Ben-Naceur et al, 1989), there is a natural limitation on the amount of acid spent near the well bore.

Three approaches to permeability enhancement by acid treatment of VMF (V*) samples were tested:

- Acid flushing.
- Acid flushing with core under confining pressure.
- Acid treatment of a refractured mineralized fracture.

Acetic acid rather than HCl was used in order to avoid complications that could arise if iron and aluminum become solubilized as hydrated cations and later precipitate as gels when the acid becomes spent.

Acid Flushing

Plugs in the V* orientation were flushed with acetic acid in an apparatus described previously (Morrow, et al., 1988). Table 3 shows the results of permeability measurements before and

Acid Flow With Core Under Confining Pressure

In the next test, the effect of acetic acid flow on permeability was investigated for a core held under confining pressure. The test plug was cut from MWX-3 Q-CO with V* orientation. The plug was saturated with brine which was then displaced by 20% acetic acid with the confining pressure set at 5,000 psi. Water permeabilities of low permeability sandstones are always much lower than gas permeabilities. Brine permeability was very low at first ($\sim 0.3 \mu\text{d}$). During the course of the test, CO_2 was generated from the reaction between calcite and acetic acid. After flowing a total of about 17 PV of acid through the core, the gas permeability was found to be of the order of 40 md even at 5,000 psi confining pressure. Brine permeability was $60 \mu\text{d}$ at $P_{cf} = 5,000$ psi and $6,000 \mu\text{d}$ at $P_{cf} = 500$ psi. The acid treatment caused obvious development of heterogeneity in the mineralized region. The core showed a distinct gap of about 1 mm caused by removal of calcite on the out-flow side of the fracture and erosion of the fracture on the upstream side.

The response of foam flow rate to decrease in confining pressure suggests that maintenance of low effective stress (high pore pressure in the formation) during acid treatment is desirable for achieving increased fracture conductivity. CO_2 foams will probably not form at reservoir pore pressures but evolution of CO_2 on release of pressure may help clean up. Fracturing with an acidized foam is still a possibility. Results obtained at high confining pressure probably correspond to the worst case for acid treatment.

Acid Treatment of a Refractured Mineralized Fracture

A V* plug from MWX-3 Q-CO was fractured along the plane of the calcite filling, with the aid of a chisel, to simulate a hydraulic fracture along the VMF. The two halves of the core were realigned and remounted in the permeability apparatus.

Permeability vs. confining pressure plots before and after fracturing are shown in Fig. 9. Fracturing resulted in about a fifteen-fold increase in permeability, but the PSR was 5.4 after fracturing, as compared to 4.6 before fracturing. The similarity of these values is probably coincidental, but may be worth noting.

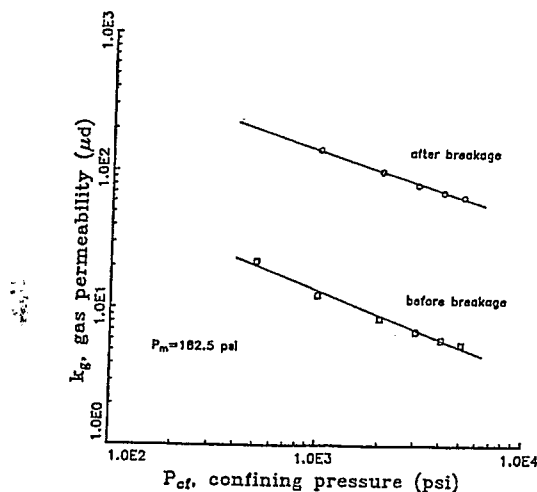


Figure 9. Effect of Breakage Along Plane of Calcite-Filled Fracture.

The fractured core sample was saturated with (8% KNO_3) brine. Following measurement of brine permeability ($k_b = 2 \mu\text{d}$ at $P_{cf} = 5,000$ psi), the brine was displaced with acetic acid. After injection of about 10 PV of acetic acid, a steady increase in volumetric flow rate was observed, and after injection of about 50 PV, evolution of CO_2 gas resulted in a rapid increase in volumetric flow rate at the outlet (see Fig.10). After flowing about 250 PV of 20% acetic acid solution through the cores it was flushed with brine. Liquid permeability was found to have increased by two orders of magnitude at high overburden pressures. Reduction of confining pressure from 5,000 to 500 psi caused the brine permeability to increase (see Fig. 10) from about 100 μd to a final value of over 1,000 μd .

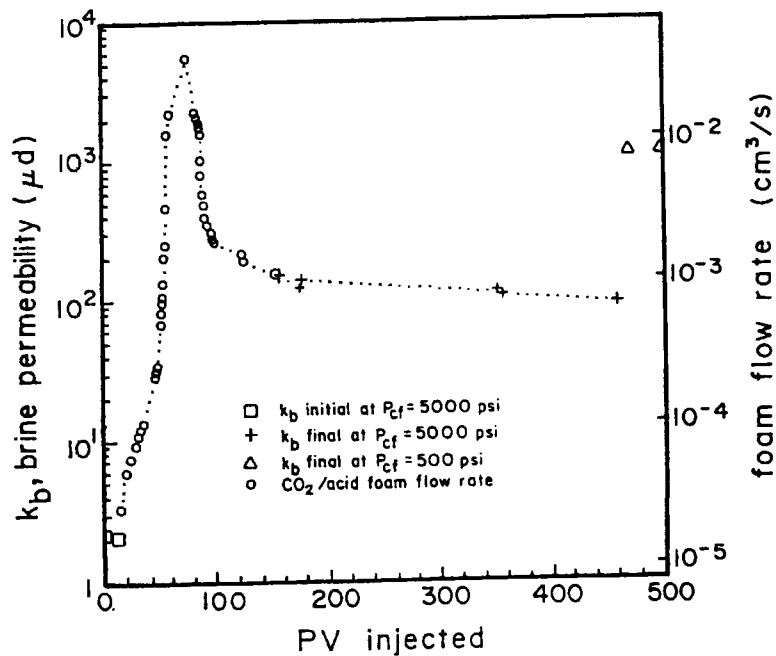


Figure. 10. Brine Permeability for Injection of Acetic Acid.

Summary

The work on VMF samples has resulted in the following conclusions:

- Plugs containing VMF's running parallel to their axis are more permeable than the neighboring matrix but usually by much less than an order of magnitude.
- VMF's do not present a barrier to crossflow.
- Pressure sensitivity of permeability to confining pressure of matrix and VMF samples is similar.
- Relative permeability measurements show that while gas flow will be reduced as water saturation increases, gas flow along a fracture relative to the matrix will be greatly enhanced by the effects of capillarity on water distribution.
- A combination of hydraulic fracturing and acidization of calcite-filled fractures provides an approach to stimulation of sand intervals such as those found in the fluvial zone of the MWX.

7. FUTURE WORK:

- Advanced core analysis and petrographic analysis will continue for selected MWX samples.
- Fluorescent dye-staining techniques will be used to determine visually effects of increased overburden pressures on pore structure.
- Further testing of relationships between permeability, pressure sensitivity, and pore structure for selected cores from various diagenetic facies will be done.
- Additional work on effects of acetic acid on permeability and pressure sensitivity of calcite-filled fractures is in progress.
- Additional work using HCl, NaOH, and oxalic acid to determine what diagenetic minerals are most important in controlling fluid flow through rock matrix is under way.
- Additional cores will be tested to determine relationship of formation factor and confining pressure to brine permeability.
- Visualization of liquid and gas phase distribution in low permeability gas sands will be attempted using fluorescent dyed styrene.
- Imbibition measurements for liquids at several levels of overburden pressure will be reported for selected MWX cores.

8. REFERENCES:

- Ben-Naceur, K., Economides, M.J., and Schlumberger, D.: "Design and Evaluation of Acid Fracturing Treatments," paper SPE 18978 presented at the 1989 SPE Joint Rocky Mountain Regional/Low Permeability Reservoirs Symposium and Exhibition, Denver, CO, March 6-8.
- Brower, K.R. and Morrow, N.R.: "Fluid Flow in Cracks as Related to Low Permeability Gas Sands," SPEJ (April 1985) 191-201.
- Finley, S.J. and Lorenz, J.C.: "Characterization and Significance of Natural Fractures in Mesaverde Reservoirs at the Multiwell Experiment Site," paper SPE 19007 presented at the 1989 SPE Joint Rocky Mountain Regional/Low Permeability Reservoirs Symposium and Exhibition, Denver, CO, March 6-8.
- Jones, F.O. and Owens, W.W.: "A Laboratory Study of Low-Permeability Gas Sands," JPT (September 1980) 1631.
- Kilmer, N.H., Morrow, N.R., and Pitman, J.K.: "Pressure Sensitivity of Low Permeability Sandstones," J. Pet. Sci. & Eng. (August 1987) 1, 65-81.
- Lorenz, J.C., Branagan, P., Warpinski, N.R., and Sattler, A.R.: "Fracture Characteristics and Reservoir Behavior of Stress-Sensitive Fracture Systems in Flat-Lying Lenticular Formations," paper SPE 15244 presented at the 1986 Unconventional Gas Technology Symposium of Pet. Eng., Louisville, KY, May 18-21.
- Morrow, N.R., Buckley, J.S., Cather, S.M., and Brower, K.R., "Rock Matrix and Fracture Analysis of Flow in Western Tight Gas Sands - Phase III," 1987 Annual Report to the U.S. Dept. of Energy, DE-AC21-84MC2119 (March 1988).
- Warpinski, N.R.: "Dual Leakoff Behavior in Hydraulic Fracturing of Tight, Lenticular Gas Sands," paper SPE 18259 presented at the 1988 SPE Annual Technical Conference and Exhibition, Houston, TX, October 2-5.

DEVELOPMENT OF CORE ANALYSIS PROCEDURES
USING X-RAY COMPUTERIZED TOMOGRAPHY

1. CONTRACT NUMBER: DE-FC21-87MC24156

CONTRACTOR: TerraTek, Inc.
360 Wakara Way
Salt Lake City, UT 84108
(801) 584-2474

PROJECT MANAGER (CONTRACTOR): John C. Sharer

PRINCIPAL INVESTIGATORS: John C. Sharer

METC PROJECT MANAGER: Karl-Heinz Frohne

PERIOD OF PERFORMANCE: August 19, 1987 to August 18, 1989

2. SCHEDULE/MILESTONES:

	Program Schedule							
	1987	1988			1989			
	<u>4thQ</u>	<u>1stQ</u>	<u>2ndQ</u>	<u>3rdQ</u>	<u>4thQ</u>	<u>1stQ</u>	<u>2ndQ</u>	<u>3rdQ</u>
Task 1 - Matrix Porosity			_____					
Task 2 - Fracture Porosity				_____				
Task 3 - Stress Effects on Porosity					_____			
Task 4 - Two Phase Relative Permeability						_____		
Task 5 - Multiphase Flow							_____	

3. OBJECTIVES:

The objective of this project is to develop procedures and analytical capabilities to evaluate core using X-ray computerized tomography. Specific analyses to be developed are:

- Matrix Porosity.
- Fracture Porosity.
- Effects of Stress on Fractures.
- Two Phase Steady State Relative Permeabilities.

- Multiphase Flow.

4. BACKGROUND

X-Ray CT was first developed as a radiological imaging technique in Great Britain by Hounsfield in 1974. This new technique was developed to allow improved resolution and three-dimensional perspectives of human bodies as opposed to more conventional radiological techniques. CT scanners generate cross-sectional images of an object by revolving an X-ray source around an object and by measuring the corresponding X-ray attenuation. From a set of these data, cross-sectional images are reconstructed by a back projection algorithm. Three-dimensional images can be reconstructed from a sequence of cross-sectional images as the object is moved through the scanner.

As X-rays pass through material, they are either scattered as they pass through the material, absorbed by the material or are attenuated. These are grouped under a general attenuation term in Beer's law. The term linear attenuation coefficient (μ), is defined in this relationship and is the basic property that is measured in X-ray computer topography scanning (CT scanning). Beer's law assumes a well collimated beam and a monochromatic source of X-rays.

In medical or industrial applications, X-rays are rarely used to pass through one "pure material, but in fact pass through multiple layers of very heterogeneous types of materials. These principles are also used in CT technology. When a test sample is inserted in a scanner, an X-ray source and detector are passed in parallel planes past the sample (called a traverse). This is repeated through a 180 degree rotation. With this data, a cross-sectional image of the test sample can be generated by dividing the sample up into small discrete elements of pixels by solving a set of linear equations. The linear attenuation coefficient for each element can be determined.

As mentioned previously, a cross-sectional image of a test sample is divided into an array of elements or pixels. As shown in Figure 1, a typical array of pixels can be 256 x 256 in size. The thickness of the collimated X-ray beam determines the thickness of the slice of material evaluated. That slice thickness then determines the volume of material (voxel) for which linear attenuation coefficients are calculated. Also, by taking multiple slices of a test sample, three-dimensional arrays of data are collected and profiled such that reconstruction of the image in any two-dimensional plane can be provided.

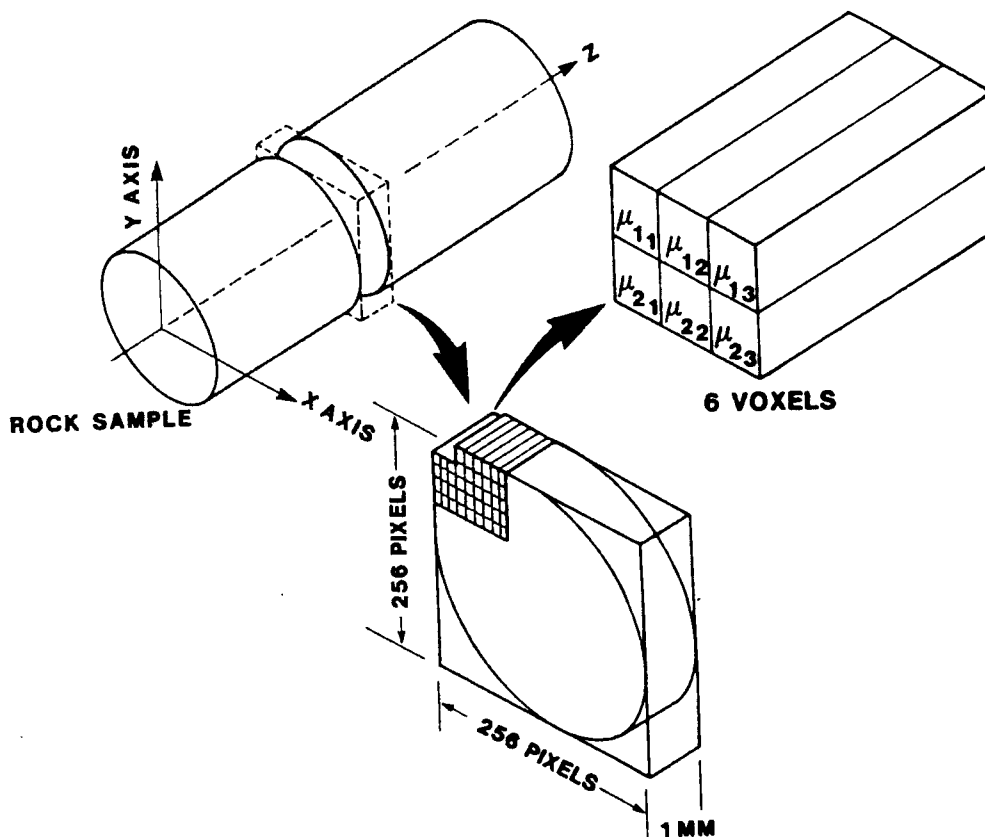


Figure 1 - CT Imaging

These arrays of linear attenuation coefficients can help in providing valuable information about the sample of interest. The attenuation of X-rays is affected by photoelectrical absorption and by Compton scattering. Photoelectric absorption is dependent on the electron density (bulk density) and the effective atomic number of the material and is predominant term at X-ray energies below 100 kV. Compton scattering is dependent on the density of material and becomes a more predominant term at energy levels above 100 kV. Therefore, the linear attenuation coefficient of a material is a function of the density and effective atomic number of the sample material and the energy level of the X-ray. This relationship is described as follows:

$$= p(a + bZ^{3.8}/E^{3.2})$$

where:

- = linear attenuation coefficient of the material
- p = density of the material
- Z = effective atomic number
- E = X-ray energy level
- a = Klein-Nishina coefficient
- b = constant

By scanning at two different energy levels (dual energy scanning), profiles of both density and effective atomic number can be attained. This procedure is, however, limited to systems where sufficient X-ray attenuation can be attained at low X-ray energies (under 100 kV). This can provide very meaningful information and drastically varying images for the same simple slice.

5. PROJECT DESCRIPTION:

It is important to note that CT scanning is not a panacea for all measurements required in the core analysis area. Direct measurements of bulk density and effective atomic number can be measured. Other measurements, such as those explored in this project, require some form of contrast and then the analytical capabilities to sort out that contrast and generate quantitative numbers.

TerraTek's CT Facility was designed and constructed before this project was initiated. It includes a modified second generation medical head scanner, a Delta-100 scanner made by Technicare. A PDP 11/04 computer is used for data acquisition. A computer controlled positioning table ties into the scanner and provides for automated data collection at specified scanning frequencies and X-ray energy level. A MicroVax II computer provides for data analysis and data output is done on a thermal graphics printer.

Each task was investigated separately and the following discusses the analysis performed.

MATRIX POROSITY

To determine matrix porosity, variations in images must be detected which exceeds the special resolution of the scanner (i.e. pore size is smaller than the dimensions of a voxel). However, if the porosity of a sample is filled with one fluid (and scanned) and then filled with another fluid with contrasting attenuation coefficient (and scanned), the difference in the two images can give a measure of porosity. Assuming a homogeneous sample of 10% porosity, each voxel will have an attenuation coefficient equal to 90% of the attenuation coefficient of the rock plus 10% of the attenuation coefficient of the fluid filling the porosity. Two fluids with contrasting attenuation coefficients can then provide data to determine porosity.

Figure 2 shows the results of scanning a visually homogeneous sandstone. Scans were taken every millimeter along the 4" diameter, 4" long core. The two fluids used were air and xenon. Variations in porosity were measured ranging from 16.4% to 20.6% which were unexpected. Unfortunately, there are no ways of cross checking each of the data points because the sample size of the CT data is too small to measure any other way. The experiment was run several times and was repeatable. The average porosity for the sample was determined to be 18.8% which corresponded well with a 18.9% Boyle's Law determined porosity.

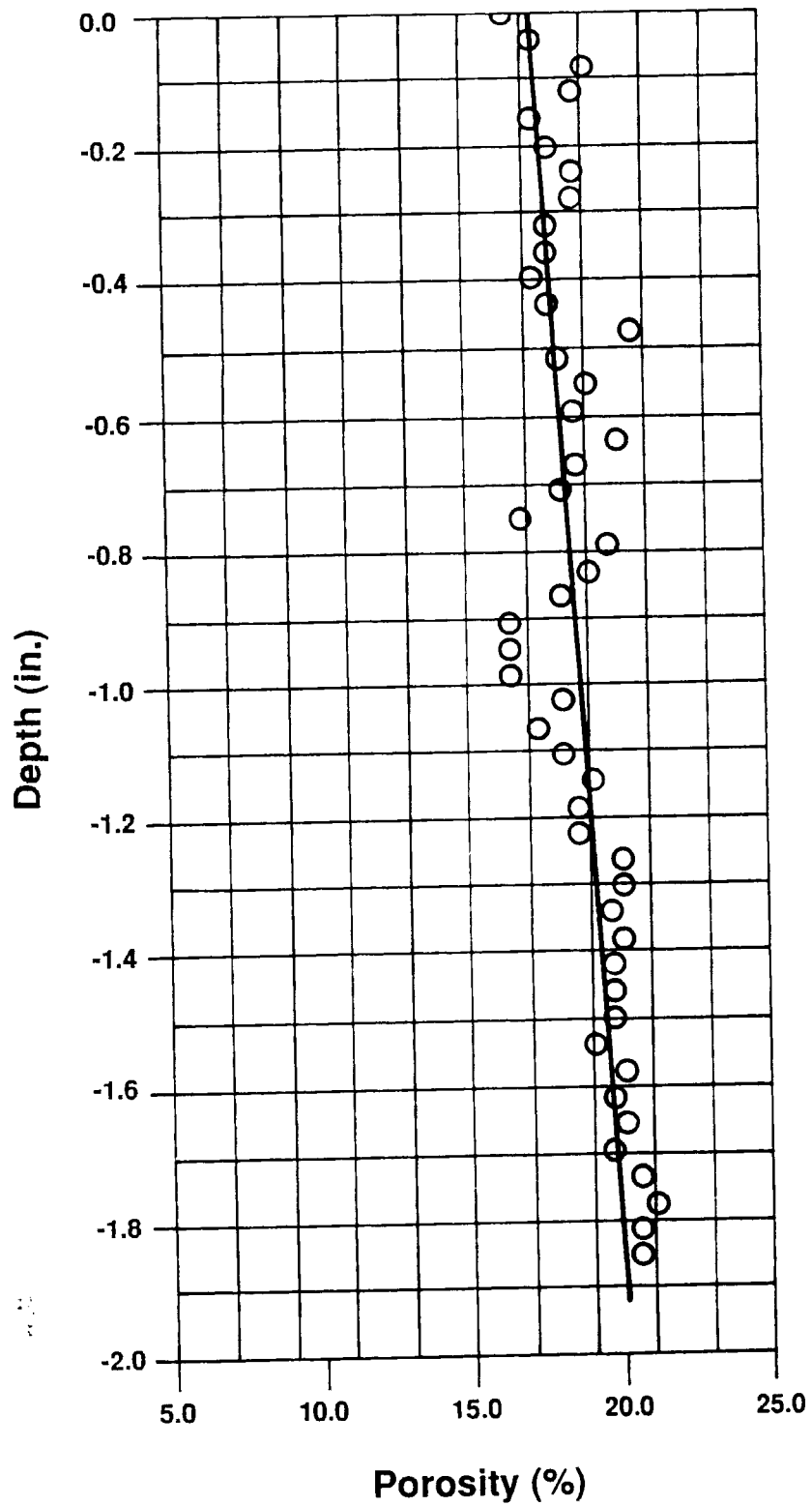


Figure 2 - Matrix Porosity Plot versus Depth for 4" Diameter x 4" Long Sandstone Sample

Repeated experiments show similar results of typically averaged measured porosities of $\pm 0.1\%$ (porosity units). The accuracy of these measurements is however dependant on the porosity of the sample, the contrast in attenuation coefficients of the fluids and the care by which the samples are saturated.

FRACTURE POROSITY

The contrast provided in fracture porosity determinations is direct measurements of bulk density and/or effective atomic number variations. To assist in quantifying fracture porosities, a masking routine was developed that converts very complex images (254 color shades) to simpler four component images. These masked images clearly delineate missing pieces of core, open fractures and vugs, filled fractures or high density mineral inclusions and the rock itself. The masking routine allows the operator to select ranges of CT numbers and then assigns one of four colors to that range. Statistical analysis is then easily performed on the number of pixels in each range.

Figure 3 shows three examples. Cross sectional images are shown in the left hand column. Masked images are generated on and shown in the middle column. They are generated by just defining a region of interest (ROI) that will be investigated. A range of CT numbers that correspond to missing pieces of core is selected and assigned black as the color designation. A range of low density (open fractures or vugs) is assigned the color blue. Areas of high density (filled fractures or high density mineral inclusions) are assigned the color red. Remaining pixels are assigned the color yellow and represent the rock itself. Statistical information on percentages of pixels in the ROI that are in each color range are then calculated and shown in the right hand column. Figure 3 shows three different rock core types with delineation of vugs, open fractures, filled fractures and high density mineral inclusions.

Resolution can become a significant problem in visually observing and quantifying fractures. In evaluating 4 inch diameter core, a field of view of about 6 inches is used in the scanner. This field of view is then divided into the 256 x 256 matrix of data. Therefore, each pixel is approximately 0.025 inches x 0.025 inches. Fractures smaller than these pixel dimensions are not clearly distinguishable and in some cases, depending on the heterogeneity of the rock, fractures larger than this are difficult to discern. Therefore, some degree of uncertainty must be noted for this type of analysis.

EFFECTS OF STRESS ON FRACTURES

The analytical capabilities for this task were generated but not studied in great detail. A flow vessel was built that provided for scanning of core under confining pressure. To determine the effects of stress on fractures. A sample is placed in the flow vessel and scanned. Masked images are generated to determine fracture porosity. Confining pressure is then applied to a designated level and the core rescanned. Masked

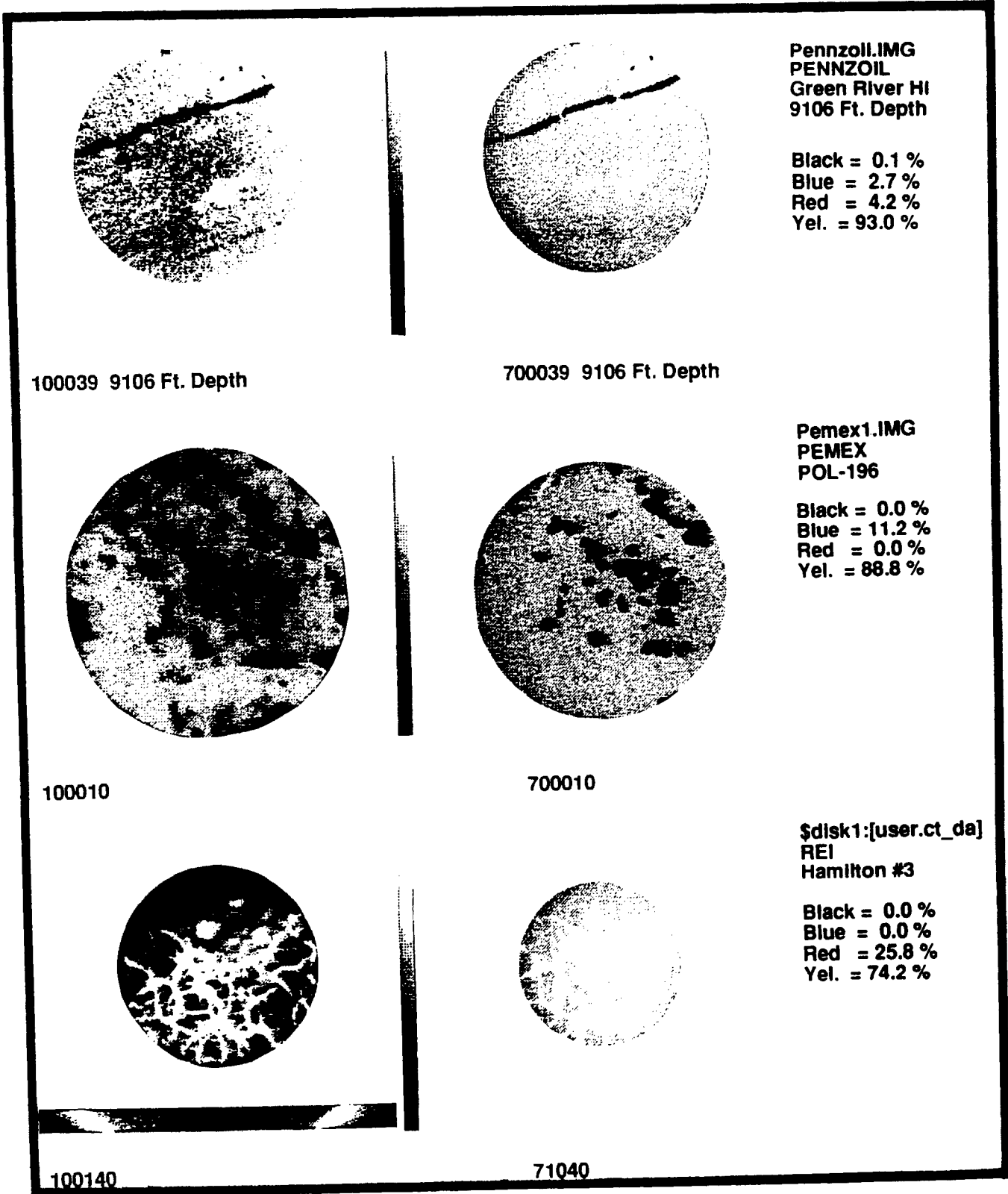


Figure 3 - Examples of Masking Routine for Three Different Rock Core Samples

images can then be generated and compared with the original data. Increasing confining pressure can be applied and results monitored.

In this case, subtractive imaging can be used to increase spacial resolution. However, limits on resolution as discussed in the previous task are still of concern. In addition, TerraTek's present capability only provides for vessels with pressure limitations of 2500 psi confining pressure. Commercially available vessels up to 10,000 psi are however available.

TWO PHASE STEADY STATE RELATIVE PERMEABILITY

Two phase steady state relative permeability measurement capabilities were also developed using a flow vessel set up for 1 1/2 inch diameter core. Pressure taps were included in the design of the vessel to measure the pressure differential from the front face of the sample to the back place of the sample. Core plugs are used on both ends of the sample to minimize capillary end effects during the testing.

The scanner is used to measure saturation profiles along the length of the sample. This capability can be used in a number of different modes. First, three dimensional profiles of fluid flow can be collected to show flow paths for samples that are not at equilibrium for certain inlet flow conditions or for heterogeneous samples. Second, the saturation profiles can help and determine equilibrium conditions for a set of flowing conditions in a sample. Third, the saturation profiles can be used to determine average saturations of a sample at equilibrium for a steady state relative permeability tests.

A typical procedure is to load a clean dry sample in the flow vessel, apply confining pressure and vacuum saturate the sample with one fluid (brine for example). The sample is then scanned from one end to the other (i.e. a series of cross sectional images). A second fluid (oil for example) is then flowed until equilibrium is attained. The sample is then rescanned. Various mixtures of the two fluids are flowed through the sample until equilibrium is attained at each step followed by scanning of the sample. This is typically done by increasing the concentration of the first fluid until the inlet concentration of the first fluid reaches 100%. The sample is then cleaned in the vessel and resaturated with the fluid and scanned. Pressure measurements are taken continuously during the test and documented on a strip chart recorder or X-Y plotter.

By knowing the attenuation coefficient profile of the sample when it is 100% saturated with the first fluid and 100% saturated with the second fluid, three dimensional profiles of saturation levels can be determined at all stages of the experiment. It is important to note that the contrast in attenuation coefficients of the two fluids and the porosity of the sample will determine the accuracy of the saturation determination. In oil/water systems the contrast is typically not great

enough for accurate saturation determination. Therefore, either phase can be "doped" with an iodated compound to provide sufficient contrast to give 1.0% saturation level accuracy.

Figure 4 shows a typical output for an endpoint saturation profile along the length of a sample for an oil/water steady state relative permeability test. Figure 5 shows an output from a fluid mobility test where a high viscosity oil is displacing a brine.

MULTIPHASE FLUID FLOW

The development of three phase fluid saturation profiling is a logical extension of the two phase analysis discussed above. Work is now underway. No results are available at the time of writing to report.

6. ACCOMPLISHMENTS:

The accomplishments of this project to date can be summarized as follows.

- Developed a measurement technique that can profile porosity variations in a sample at intervals as small as 1 mm. Average porosity measurements for an entire sample are within ± 0.1 porosity units of measurements using the classical Boyle's Law technique.
- Developed masking routine to profile fracture porosity (filled and unfilled) in rock core. Fractures must be at least 0.25 inches in width. Profiles of high density mineral inclusions can also be determined.
- Fractures have been analyzed under stressed and unstressed conditions using analytical capabilities to determine changes that are developed.
- Two phase steady state relative permeability procedures have been developed that can accurately determine saturation profiles in core to a 1% saturation level. Commercial services have been provided to a number of clients using this technique.

7. FUTURE WORK:

Future work under this existing contract will include the completion of the last task dealing with saturation profiling of three phase flow. Other areas of interest that require additional study deal with the study of fluid flow in three dimensions in heterogeneous types of rock to sort out fracture permeability and matrix permeability.

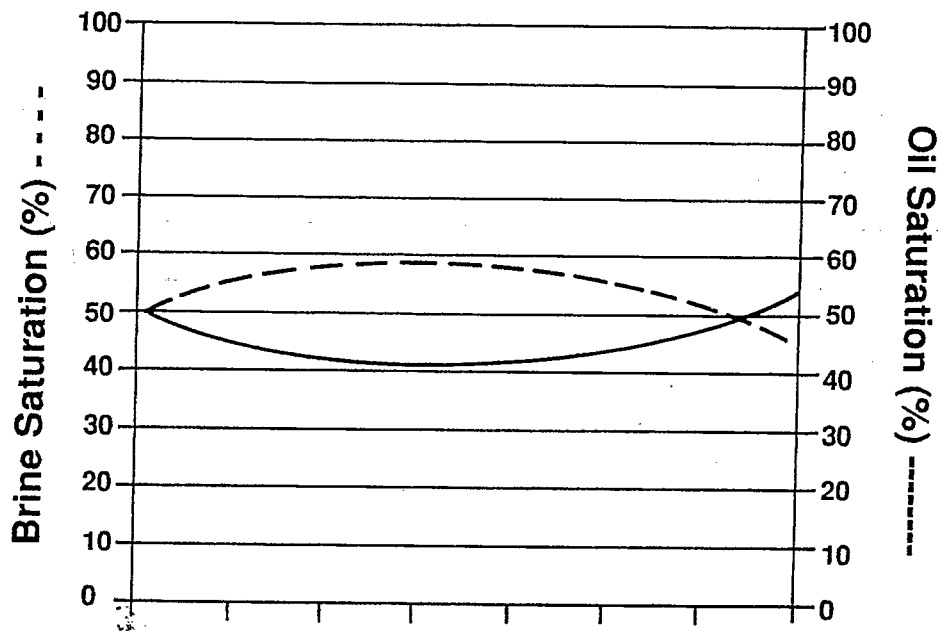


Figure 4 - Saturation Profile for Core After 70% Oil/30% Brine Inlet Flow Attained Equilibrium

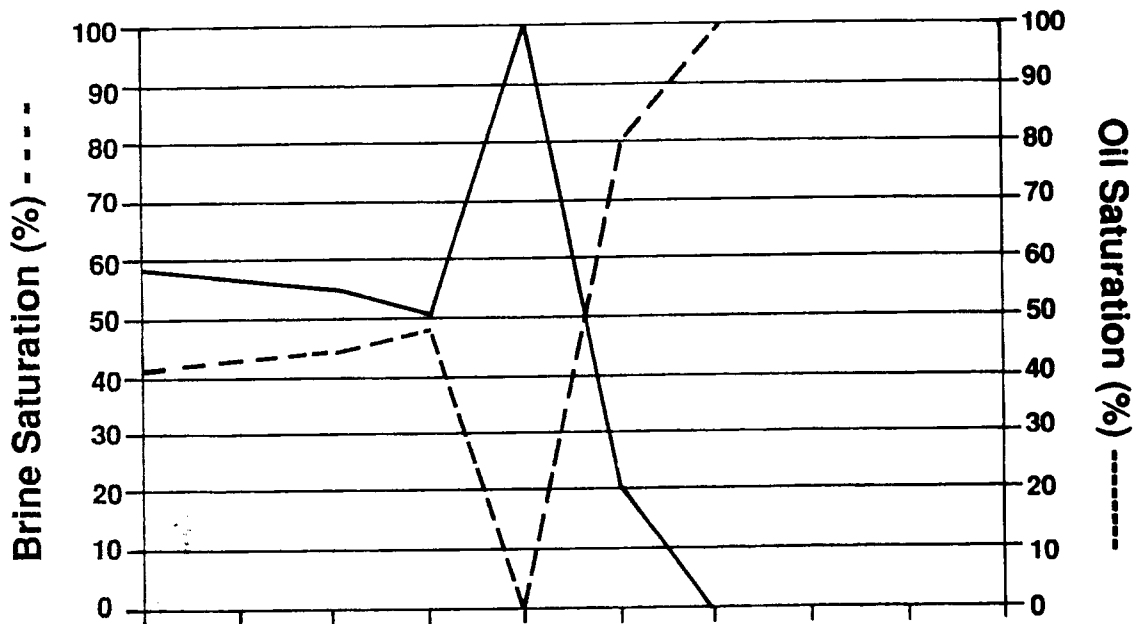
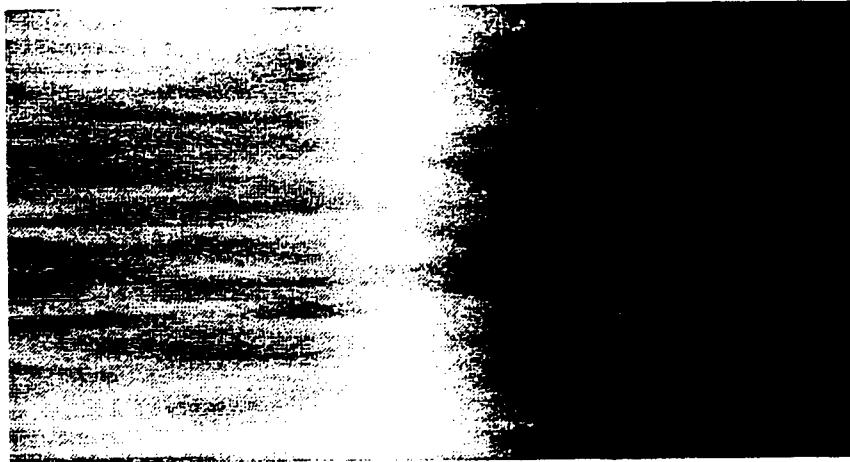


Figure 5 - Saturation Profile for Flow Dynamic Studies

8. REFERENCES:

Barrett, H.H. and Swindell, W.: Radiological Imaging, Academic Press, New York City (1981).

Brooks, R.A. and DiChiro, G.: Principles of Computer-Assisted Tomography in Radiographic and Radioisotopic Imaging, Phys. Med. Biol. (1976) 21, 689-732.

Evans: The Atomic Nucleus, McGraw-Hill Book Co., New York City (1955).

Hounsfield, G.N.: A Method of and Apparatus for Examination of a Body by Radiation Such as X- or Gamma-Radiation, British Patent No. 1,283,915, London (1972).

Reconstruction Tomography in Diagnostic Radiology and Nuclear Medicine, M. Ter-Pogossian, M.M. Phelps, and G.L. Brownell, (eds.), University Park Press, Baltimore (1977).

Wellington, S.L. and Vinegar, H.J., X-Ray Computerized Tomography, Journal of Petroleum Technology, August 1987, Vol. 39, No. 8, pp. 885-898.

TWO-PHASE FLOW IN TIGHT SANDS

1. CONTRACT NUMBER: DE-FG21-85MC22000

CONTRACTOR: Institute of Gas Technology
3424 South State Street
Chicago, IL 60616
(312) 567-3650

CONTRACTOR PROJECT MANAGER: Prasan Chowdiah

PRINCIPAL INVESTIGATOR: Prasan Chowdiah

METC PROJECT MANAGER: Karl-Heinz Frohne

PERIOD OF PERFORMANCE: September 30, 1985 to September 29, 1987

2. SCHEDULE/MILESTONES:

The first year of the contract period was devoted mainly to developing experimental procedures for two-phase flow measurements in tight sands. A significant amount of data, primarily on Mesaverde sandstones, was collected and analyzed during the second year and used to develop guidelines for the use of relative permeability curves as inputs in reservoir simulation.

3. OBJECTIVES:

The objective of this project was to develop equipment as well as laboratory and analytical techniques for obtaining properties of tight sands that are needed for two-phase computer simulation of production. In this context the desired properties are capillary pressure, permeability to gas and permeability to water as functions of water saturation. Emphasis was on conducting experiments under net stresses representative of in-situ stress levels, and on developing techniques whereby water saturation in the sample can be varied under controlled conditions of drainage or imbibition rather than by evaporation.

4. BACKGROUND STATEMENT:

Most conventional core analysis techniques used for high permeability sandstones are not readily applicable to tight sandstones, primarily due to the extremely small flow rates and high capillary pressures encountered in these sandstones. Owing to these problems, much of the data on two-phase flow permeabilities in tight sands is obtained using evaporation to vary water saturation. Also, capillary pressures are measured using the mercury porosimetry and the centrifuge techniques, neither of which adequately simulates reservoir confining stress. In contrast, what the reservoir engineer needs as matrix property inputs for computer simulation are true drainage and imbibition relative permeability curves and capillary pressure curves at reservoir net stress. Therefore, there is a need to develop laboratory and analytical

techniques that will provide reliable estimates of tight sand properties at in-situ conditions.

Efforts at addressing some of the above problems were begun at IGT under sponsorship from the Gas Research Institute, and an apparatus called the Experimental Tight Rock Apparatus (EXTRA) was built for making related measurements (Chowdiah 1987a). This project enabled continuation of the work begun under GRI sponsorship.

Prior to the start of this project, some preliminary experiments had been conducted on measuring true drainage capillary pressure and relative permeability data under in-situ stress conditions. During the course of this project, work continued on improving these experimental techniques, together with the development of new procedures that permit more rapid estimation of some reservoir properties.

5. PROJECT DESCRIPTION:

Figure 1 shows a schematic of the sample assembly in the EXTRA, which was used for the experimental work. The feature of the EXTRA that permits drainage experiments is that the downstream end cap in the coreholder provides separate outlets for gas and water, and has provision for using a capillary barrier in contact with the sample to separate the two phases. The downstream gas pressure can be adjusted to any desired value while the water exits into a pipet that is open to the atmosphere.

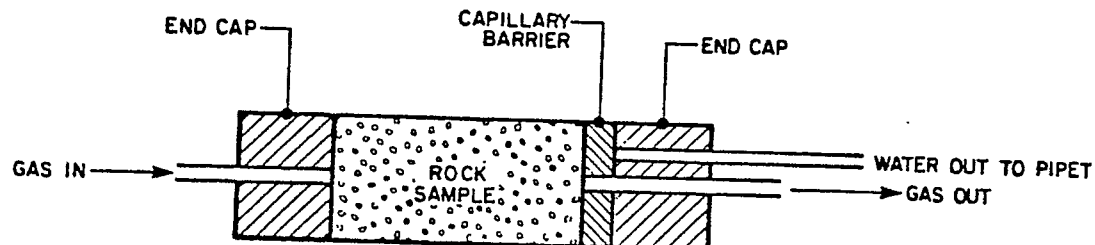


Figure 1. Schematic of Coreholder Assembly

Early in the project, coordinated measurements of capillary pressure and gas phase relative permeability under drainage conditions at reservoir net stress were made. However, these measurements were found to be excessively time-consuming, requiring upwards of eight weeks per capillary pressure curve.

Later in the project the experiments were modified to concentrate on measuring water permeability, gas entry capillary pressure, critical gas saturation and gas phase permeability at gas saturations just above critical. The idea was that these parameters should yield sufficient information to enable reasonable estimation of capillary pressure and relative permeability curves at in-situ conditions. Measurements were made on 10 Mesaverde tight sand samples and one sample from the Frontier formation. The results were analyzed to come up with a set of guidelines or "rules-of-thumb" which should prove useful for estimating reservoir

matrix relative permeability inputs for computer simulation in the absence of detailed laboratory data.

6. RESULTS/ACCOMPLISHMENTS:

All laboratory data were obtained using nitrogen and distilled water as the flowing phases. "Dry" sample properties used in data analysis refer to samples dried to equilibrium at 45% relative humidity and 60°C. Results are outlined below under specific headings.

CAPILLARY PRESSURE

Gas-water capillary pressure curves at reservoir net stress conditions were measured using a "thirsty" glass capillary barrier and compared with results from mercury penetration data on unconfined sample chips (Chowdiah 1986). The results showed a significant shift in capillary pressure curve due to the effect of confining stress. However, the extent of this stress-effect is dependent on the pore morphology of the rock.

SPECIFIC WATER PERMEABILITY

Correlation With k_{∞}

Figure 2 shows a plot of water permeability k_w versus Klinkenberg permeability k_{∞} for the present data set. Different symbols have been used to identify samples based on their depositional environment. The Mesaverde fluvial, coastal and paludal sandstone samples are denoted by a cross, circle and triangle respectively, while the Frontier sandstone sample is denoted by a diamond. Also shown by a dashed line in the plot is a correlation developed by Jones and Owens (1980). The equation for this line is:

$$k_w = k_{\infty}^{1.32} \quad (1)$$

where both k_w and k_{∞} are in millidarcies.

It can be seen that the present data lie predominantly below the correlation given by Equation 1. The solid line is the best fit regression line through the data points. However, the difference between the two lines is small for a correlation of this type, particularly towards the higher end of the permeability scale in Figure 5, which is likely to be the region of interest from the perspective of gas production from tight sands. Therefore, though the present data lie slightly below the dashed line, they are close enough to justify the use of the Jones and Owens' correlation (Equation 1) as a generalized correlation for tight sands.

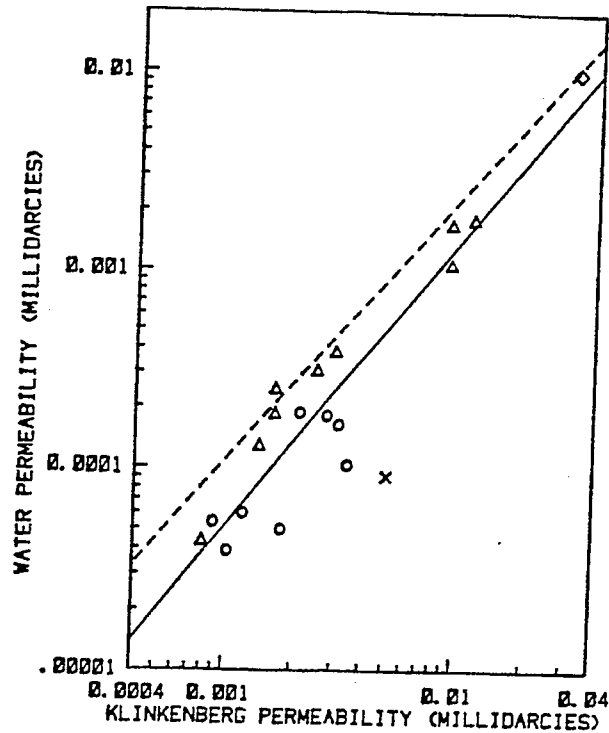


Figure 2. Specific Water Permeability vs. Klinkenberg Permeability

Correlation With k_{rg} Data

The relationship of measured specific water permeabilities to gas phase relative permeability data was studied with the objective of shedding some light on the large difference observed between specific water permeability and specific gas (Klinkenberg) permeability in tight sands. Data of effective gas phase permeability versus water saturation for the samples being studied had been measured earlier (Randolph et al. 1985, Chowdiah 1986). These data were used to determine the water saturation at which the effective gas phase permeability equaled the specific water permeability for each sample. Results showed that this water saturation was in the neighborhood of 40% for all the samples. This result is intriguing, particularly since the samples spanned a Klinkenberg permeability range of 1 to 30 microdarcies, and the ratio of specific water permeability to Klinkenberg permeability for the samples varied from as low as 0.03 up to a value of 0.3.

The water saturation value around 40% is close to the irreducible water saturation that one might expect in tight sands. Desorption data, obtained by drying tight sand samples to equilibrium at different relative humidities in a controlled humidity chamber (Ward and Morrow 1985; Chowdiah 1987), show that adsorbed water can account for as much as 20% of the pore space. Jones and Owens (1980) found that displacement of water from tight sands by gas drive using an injection pressure of 1000 psi reduced water saturation to an average of 40% pore space. They also observed that effective gas permeability obtained after water

displacement was close to the specific water permeability. The present data which are in agreement with earlier results of Jones and Owens, suggest that irreducible water saturations in tight sands are in the neighborhood of 40% pore space, and that effective gas permeability at irreducible water saturation equals the specific water permeability. This is a potentially very useful conclusion since the irreducible water saturation is an important input parameter in modeling the performance of a reservoir.

GAS ENTRY PRESSURE

Gas entry capillary pressure for the samples was measured using the arrangement shown schematically in Figure 1. A capillary barrier of 1/8-inch thick porcelain having a gas entry pressure of approximately 5 psi was used. Downstream gas pressure was maintained at about 1 psi above atmospheric so as to be below the entry pressure for the barrier. With the sample plug fully water-saturated, upstream gas pressure was increased in steps of 5 to 10 psi until the gas entry pressure was just exceeded. This was indicated by displacement of water into the downstream pipet. Gas breakthrough to the downstream end of the plug was indicated by a sudden increase in downstream gas flow rate from a value close to zero. Details of the experimental procedure are available in Chowdiah (1987b, 1988).

Figure 3 shows a plot of measured gas entry capillary pressures at initial reservoir net stress versus entry pressures estimated from mercury porosimetry data. The mercury entry pressures were divided by a factor of 5 to account for differences in interfacial tension and contact angle between the mercury-vacuum and gas-water systems. Figure 3 shows

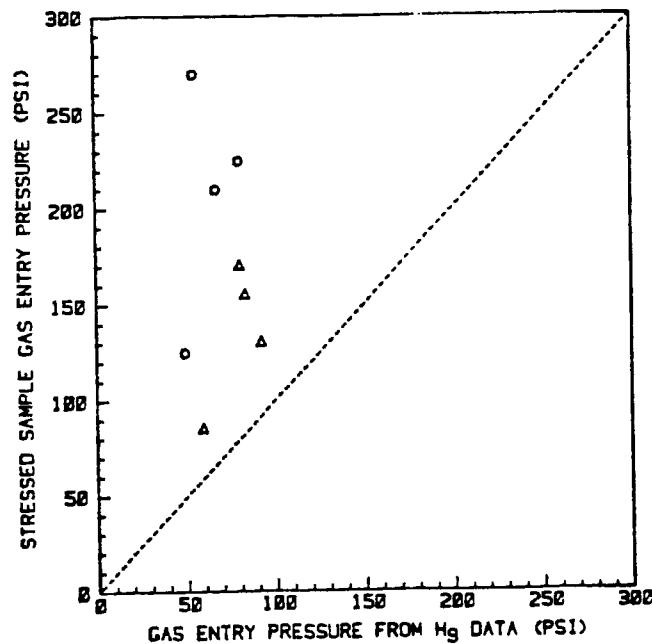


Figure 3. Effect of Confining Stress on Gas Entry Pressure

that the mercury data invariably underestimated the gas entry pressure. However, the magnitude of the difference varied. While for some samples the estimate from mercury data was quite close to the stressed sample data, for others it differed by as much as a factor of 5. The difference is attributable, at least in part, to the strong effect of confining pressure on the pore space in tight sandstones. Distortion (rounding) of the mercury capillary pressure curve near the entry region can occur due to the small size of samples used in mercury porosimetry (Swanson 1981). This can also contribute to low estimates of entry pressure, and in fact could very well be the predominant cause of observed differences for samples where the estimates from mercury data are fairly close to the confined sample values. However, for most of the samples the confining stress effect is very strong.

Figure 3 shows the coastal sample gas entry pressures (circles) to be much more stress sensitive than those for the paludal samples (triangles). This fact correlates well with earlier results for Mesaverde sandstone core analysis which showed that the coastal sands had higher pore volume compressibilities (Soeder and Randolph 1984), and also that the coastal sandstone permeabilities were more stress sensitive than the paludal (Randolph et al., 1985). The confined sample gas entry pressure measurement, in combination with mercury entry pressure data, appears to provide a good indicator of the stress sensitivity of tight sandstone properties. Measured gas entry capillary pressures at in-situ net stress could also be useful for correcting mercury porosimetry capillary pressure curves to reservoir stress conditions. Further work is needed to establish a procedure for making such corrections.

CRITICAL GAS SATURATION

Critical gas saturations were determined by the average gas saturation in the sample at the time of gas breakthrough. Results showed that critical gas saturation under drainage conditions for these tight sandstones is around 10% or less. This small critical gas saturation is in contrast to data obtained using evaporation to vary water saturation, which yield critical gas saturations around 40%. The mechanism of water redistribution during core analysis using the evaporation method is such that the pore water distribution is probably close to that during imbibition, so that "evaporation" data provides a good approximation to imbibition relative permeabilities (Chowdiah 1986).

EFFECTIVE GAS PHASE PERMEABILITY

Gas and water flow rate data were recorded for approximately one day after gas breakthrough with the upstream gas pressure held constant at a value just above the entry pressure. Thereafter, additional desaturation of the sample was obtained by imposing a step increase in upstream pressure and monitoring flow rates. These data were used to calculate the variation of effective gas phase permeability with water saturation. Gas phase permeability was calculated from gas flow rate using Darcy's law:

$$k_g = \frac{q \mu L}{A \Delta P} \quad (2)$$

where q is the gas flow rate at the mean pore pressure in the sample. This equation is strictly valid for the case of a stationary water phase. Its use here is justified by the fact that gas flow rates were from 10 to 100 times larger than the water displacement rates.

Results obtained using this procedure are illustrated in Figure 4 which shows plots of gas permeability versus average water saturation for two Mesaverde paludal samples. These plots were the result of direct, computer aided manipulation of raw data recorded by the data acquisition system, which explains the somewhat jagged nature of the curves where flow data was momentarily affected by the operation of solenoid valves in the system. Note that the abscissas in Figure 4 are restricted to high water saturations of greater than 75%, and also that the permeability scale is different for each plot. The effective gas permeabilities shown in these plots correspond to relative permeabilities (based on the dry sample Klinkenberg permeability) of the order of 10^{-3} , so that these data correspond to the tail end of the gas phase relative permeability curve, very close to the critical gas saturation.

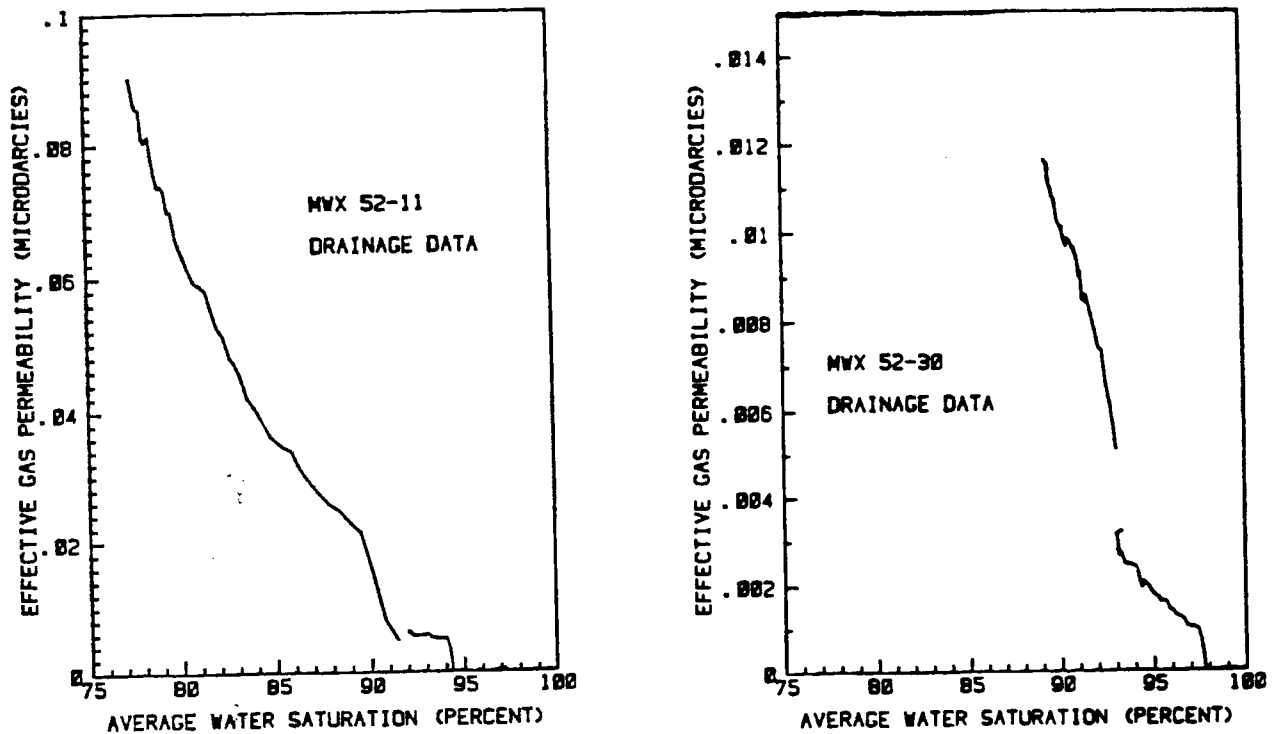


Figure 4. Effective Gas Phase Permeability Versus Water Saturation

GUIDELINES FOR ESTIMATION OF RELATIVE PERMEABILITY CURVES

In view of the difficulties involved in laboratory two-phase flow measurements in tight sands and the time consuming nature of such experiments, it often becomes necessary to estimate relative permeability inputs for computer simulation without waiting for detailed core analysis data. The results of this study have provided the following guidelines that can be used to estimate the relative permeability behavior of the matrix in a tight sand reservoir.

- Critical gas saturation (S_{gc}) can be set equal to 10% for the drainage case and 40% for the imbibition case.
- Irreducible water saturation (S_{wi}) can be set equal to 40%.
- The effective gas Klinkenberg permeability at irreducible water saturation can be assumed equal to the specific water permeability.
- Data on Mesaverde sandstones indicate that the Jones and Owens (1980) correlation is adequate for estimating specific water permeability when gas Klinkenberg permeability of a dry sample is known.
- The Swanson parameter from mercury porosimetry can be used to estimate Klinkenberg permeability of the dry rock (Chowdiah, 1986; Walls and Amaefule, 1985).

7. EVALUATION OF POTENTIAL FOR FUTURE WORK:

The results of this project have led to the identification of certain areas where further research is needed, with the objective of better and faster techniques for formation evaluation using laboratory data.

- More work is needed to quantify the effect of confining stress on capillary pressure curves, particularly from the perspective of coming up with a simple procedure for correcting mercury penetration data to reservoir stress conditions.
- Displacement experiments of the type described here can be extended to lower water saturations. However, these experiments involve significant saturation gradients in the sample. The effect of saturation gradients will have to be included and properly accounted for during data interpretation to obtain meaningful information on relative permeability curves.
- While methods have been developed for measuring gas phase permeability at different water saturations in tight sands, it is still not possible to directly measure effective liquid permeability. Future work aimed at developing techniques for making these measurements is desirable.

- Indications are that pore morphology plays an important role in determining many of the properties of tight sands and may be the critical factor in explaining the variation of these properties with depositional environment, depth of burial etc. Petrographic studies of pore morphology need to be conducted in conjunction with core analysis to develop its potential as a useful formation evaluation tool.
- Results reported here are based primarily on data obtained with Mesaverde sandstone samples. It is felt that the same or similar results should be valid for tight sands from other formations. However, a sufficient data base for verifying this assumption for other formations is not available at this time. Laboratory measurements aimed at building up a comprehensive data base is an area for future work.

SUBSEQUENT WORK UNDER GRI SPONSORSHIP

Following the conclusion of this project, IGT has been able to address the last two issues listed above under funding from GRI. Cores from the Travis Peak formation in East Texas have been analyzed using mercury porosimetry, flow studies, and petrography. Results thus far indicate that the conclusions arrived at under the DOE program for Mesaverde sandstones can be extrapolated to other formations. Much of the emphasis in the work currently being done for GRI is on the development of mercury porosimetry and petrography as useful tools for tight sand formation evaluation.

Observation of rock pore geometry from "thin sections" under an optical microscope can be performed either in transmitted light or using fluorescent microscopy. In the second approach which we have found particularly useful for tight sands, the sample is impregnated with epoxy containing a fluorescent dye. The dye in the pores fluoresces strongly under incident light of a specific wavelength, permitting even extremely small pores to be observed. Besides tight sands, this technique is also useful for opaque materials such as shale and coal. Details of the technique are available in Soeder and Chowdiah (1988).

Figure 5 illustrates the three main classes of pore geometry found in tight gas sandstones. The first class contains grain-supported primary pores and gives rise to what is basically a conventional sand made tight by precipitation of minerals in pore throats. The second class contains highly altered primary porosity, extensively filled in with authigenic minerals, usually quartz overgrowths, until it is reduced to narrow "slot" pores. This is generally coupled with significant amounts of secondary solution pore development. While most of the porosity occurs in the solution pores, the slots provide a bottleneck for fluid flow and make the rock tight. The third, and a relatively rare class consists of ultrafine microporosity in an all-pervading matrix composed of clay, carbonate or silica, in which sand-sized quartz grains are suspended. Individual tight sand samples often contain more than one class of pore geometry, although a single class

usually predominates. The slot and solution pore geometry is the most common type observed by us in tight sands, including the Mesaverde. The slots are responsible for low permeability and a high stress dependence of permeability. On the other hand, sandstones with the grain supported pore geometry are much less stress sensitive.

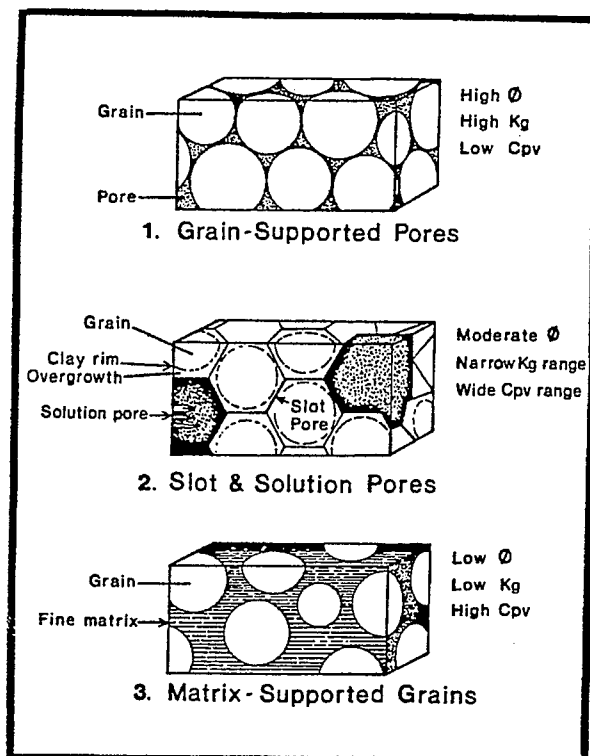


Figure 5. Classes of Pore Geometry in Tight Gas Sandstones

Figure 6 shows a plot of Swanson parameter (Swanson, 1981) from mercury porosimetry versus Klinkenberg permeability for both Mesaverde and Travis Peak sandstones. The crosses in the plot represent Mesaverde data while the other symbols have been used for Travis Peak samples from different wells. The letter "F" denotes fractured samples. It is obvious that the low permeability Travis Peak data are in excellent agreement with the Mesaverde data, suggesting that such a correlation is not formation-specific. The plot also shows the conventional sandstone correlations derived by Swanson for air permeability (dashed line) and brine permeability (dotted line). Figure 6 shows that the tight sands data lie close to Swanson's correlations at higher permeabilities but deviate significantly at lower permeabilities.

Microscopic examination has shown that the increased deviation from Swanson's correlation with decreasing permeability is explained by changes in pore geometry. The Travis Peak samples analyzed show a gradual transition from grain supported pore geometry at the high end of the permeability scale in Figure 6, to slot and solution pore geometry at the low end. The transition region is characterized by samples which show primary porosity accompanied by a partial development of slot and solution porosity. In the Travis Peak, the

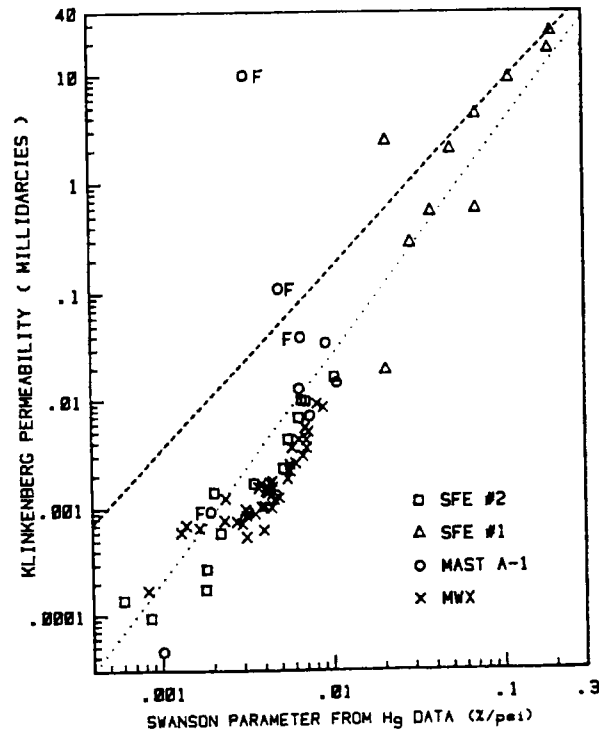


Figure 6. Permeability vs. Swanson Parameter for Mesaverde and Travis Peak Cores

degree of development of secondary porosity has been shown to correlate with depth (Soeder and Chowdiah, 1988).

8. REFERENCES:

Chowdiah, P. "Effects of Pore Water Distribution and Stress on the Laboratory Measurement of Tight Sandstone Properties," paper SPE 15210 in Proceedings of the SPE Unconventional Gas Technology Symposium, Louisville, KY, May 18-21, 1986, 35-46.

Chowdiah, P. "Measurement and Analysis of Two-Phase Flow Through Low Permeability Media. Task 2. Experimental Research," Final Report No. GRI-86/0123-1 prepared for Gas Research Institute under Contract No. 5082-260-0711, Institute of Gas Technology, Chicago, March 1987.

Chowdiah, P. "Laboratory Measurements Relevant to Two-Phase Flow in a Tight Gas Sand Matrix," paper SPE 16945 in Proceedings of the 62nd Annual Technical Conference and Exhibition of the SPE, Dallas, TX, Sept. 27-30, 1987b.

Chowdiah, P. "Two-Phase Flow in Tight Sands," Final Report DOE/MC/22000-2633, prepared for the U.S. Department of Energy, Morgantown Energy Technology Center, under Contract No. DE-FG21-85MC22000, Institute of Gas Technology, Chicago, July 1988.

Jones, F. O. and Owens, W. W. "A Laboratory Study of Low Permeability Gas Sands," J. Pet. Tech. 34 1631-40 (September 1980).

Randolph, P. L., Soeder, D. J., and Chowdiah, P. "Effects of Water and Stress Upon Permeability to Gas of Paludal and Coastal Sands, U.S. DOE Multiwell Experiment," Topical Report DOE/MC/20342-1838, prepared for the U.S. Department of Energy, Morgantown Energy Technology Center, under Contract No. DE-AC21-83MC20342, Institute of Gas Technology, Chicago, February 1985.

Soeder, D. J. and Chowdiah, P. "Comparison of Pore Geometry in High- and Low- Permeability Sandstones, Travis Peak Formation, East Texas," paper SPE 17729 in Proceedings of the SPE Gas Technology Symposium, Dallas, TX, June 13-15, 1988.

Soeder, D. J. and Randolph, P. L. "Special Dry Core Analysis of the Mesaverde Formation, U.S. DOE Multiwell Experiment, Garfield County, Colorado," Topical Report No. DOE/MC/20342-4, prepared for the U.S. Department of Energy, Morgantown Energy Technology Center, under Contract No. DE-AC21-83MC20342, by Institute of Gas Technology, Chicago, June 1984.

Swanson, B. F. "A Simple Correlation Between Permeabilities and Mercury Capillary Pressures," J. Pet. Tech., 2498-2504 (1981) December.

Ward, J. S. and Morrow, N. R. "Capillary Pressures and Gas Relative Permeabilities of Low Permeability Sandstones," paper SPE/DOE 13882 in Proceedings of the 1985 SPE/DOE Joint Symposium on Low Permeability Reservoirs, Denver, May19-22, 321-334.

APPLICATION OF STRATIFIED RANDOM SAMPLING TO ESTIMATING GAS RESERVES

1. CONTRACT NUMBER: DOE-METC/EG&G NUMBER DE-AC21-85MC21353

CONTRACTOR: EG&G Washington Analytical Services Center, Inc.
 DOE-METC
 3610 Collins Ferry Rd.
 Box 880
 Morgantown, WV 26507

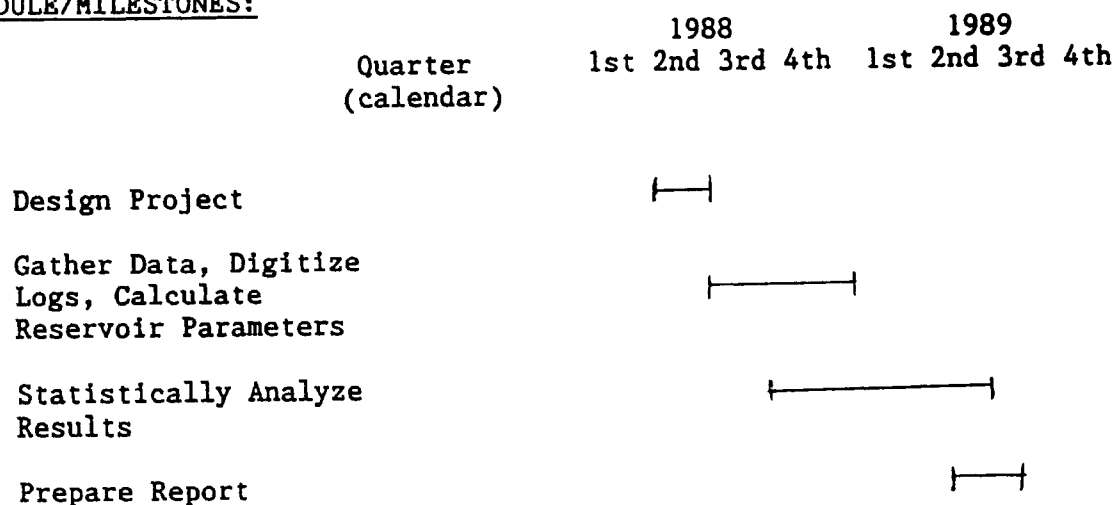
CONTRACT PROGRAM MANAGER: Keith Westhusing

PRINCIPAL INVESTIGATORS: Allan Smith
 John Hancock
 Mark Portman
 Ray Lopez

METC PROJECT MANAGER: Karl-Heinz Frohne

CONTRACT PERIOD OF PERFORMANCE: July, 1988 through September, 1989

2. SCHEDULE/MILESTONES:



3. OBJECTIVES:

The purpose of this study was to assess the usefulness of stratified random sampling in estimating reservoir parameters and to verify the porosity, net pay thickness, gas saturated pore space, and resulting gas-in-place estimates made by the National Petroleum Council (NPC,1980) for the Dakota Formation in an area of San Juan Basin.

4. BACKGROUND STATEMENT:

The volumetrics equation (Equation 1) is the most common way to estimate hydrocarbon reserves before the production and pressure histories of wells have been established. The equation is expressed in equation 1:

$$GIP = ((43.56*POR*(1-SW))/z)*(520/T)*(P/14.65)*H*A*640 \quad (1)$$

Where GIP is gas in place in MCF
POR is porosity in decimal form
SW is water saturation in decimal form
z is the gas compressibility factor (dimensionless)
T is the temperature in degrees Rankine
P is bottom hole pressure in Pounds per Square Inch Atmospheric
A is the productive area in square miles.
H is the net pay thickness in feet

The essential unknowns in this equation are porosity, net pay thickness, and water saturation. Published estimates of gas reserves for entire basins such as those done by the NPC (NPC,1980) have determined these unknowns by seeking advice from several experts in the basins studied and then inserting the expert's estimates into equation 1. This method certainly has benefits in that it is quick, cheap and often yields satisfactory results. The drawbacks of the method are that it is not reproducible, it is subject to the bias of the experts, and it has no means of quantifying the reliability of its estimates.

The present study utilizes the statistical technique of stratified random sampling to sample wells from an area in the San Juan Basin. The term stratified means that the population to be sampled is divided into sets (strata) that have similar characteristics. For example, a stratified sampling plan for a public opinion poll may group urban apartment dwellers into one strata and home owners into another strata. Random samples are then selected in each strata. This sampling method will usually give a more precise estimate (less variation in its estimates) of a population's mean value than will the same number of randomly selected samples.

The strata used in this study were government surveyed townships, most of which are 36 square miles in area. Twelve strata (townships) were randomly selected from all the strata in the study area. From these twelve strata wells were selected in a semi-random fashion and the logs of these wells were used to calculate porosity, net pay thickness, and water saturation. These values were then used in equation 1 to estimate in-place gas reserves. In anticipation of estimating recoverable gas, permeability estimates were also derived from the well logs.

5. PROJECT DESCRIPTION:

I. THE TECHNIQUE OF STRATIFIED RANDOM SAMPLING

A review of the literature has failed to show any applications of random stratified sampling in hydrocarbon resource estimation. Forestry researchers (Bertram, 1971, Bourdeau, 1953, Barton, 1956, Vries, 1986) have successfully applied the technique in estimating forest resources. These studies (Bertram, 1971, Bourdeau, 1953, Barton, 1956) have shown an effective way to stratify a population is to divide the study area into smaller areas and then randomly select samples from these small study areas. It appears that this type of sampling will provide advantages in estimating geological parameters because of the similarities in the problems being solved.

These similarities include:

- . Both are volumetric estimates of a resources over a large geographical area
- . Both have relationships between topography and resource availability.

There are also major differences between the fields of study:

- . Forestry resources change at a faster rate than petroleum resources. Tree maturation occurs faster than gas maturation.
- . Forestry parameters can be directly measured at a much finer scale than geological parameters.

Forestry studies on the bias (accuracy) of sampling methods and the variability of parameter estimates were reviewed (Bertram, 1971, Bourdeau, 1953). Studies of the effects of size and shape of the sampled area on the parameter estimates were also reviewed (Chapman 1932, Myers and Chapman 1932, Barton 1956).

A number of papers (Bertram 1971, Bourdeau, 1953, Vries 1986, Snedecor and Cochran, 1967, Hoel, 1971) addressed the relationship of the sampling method to the accuracy of study results. Systematic non-random sampling techniques (Bertram, 1971) were used in forestry surveys before the development of random sampling designs. The systematic techniques do not provide for precision estimate (Bertram, 1971). It is highly recommended that sampling error estimates be performed (Bertram, 1971). The importance of careful sampling should not be overlooked since meaningless variability and inaccurate results often accompany poor sampling techniques (Bertram, 1971). Bourdeau (1953) concluded random sample locations should be used whenever possible since random sampling increases accuracy and allows variability estimates. It was also noted (Bourdeau, 1953, Snedecor and Cochran 1967) that systematic samples may coincide with parameter periodicity which will cause very un-representative parameter estimates.

These studies (Bertram 1971, Bourdeau 1953, Vries 1986, Snedecor and Cochran 1967, Hoel 1971) strongly suggest that the random selection of study area locations will lead to the least biased and the most accurate parameter estimations. One of the major differences between the study methods typically employed by geologist and the stratified sampling method is the sample selection method. Unfortunately for many geological studies an area is picked based on the amount of available data; this selection method can easily result in the parameter values being unrepresentative of the basin. Two possible bias sources caused by the data availability selection method are:

- Areas of better than average reservoir quality are more likely to have more data than poorer areas because operators will generally have more wells in the better areas.
- A well operator may choose a particular location because careful study suggested the reservoir properties are better.

A number of papers (Barton 1956, Vries 1986, Snedecor and Cochran 1967) also compared different random sampling techniques effects on the variability of a studied parameter. All of the studies reviewed which compared (Barton 1956, Snedecor and Cochran 1967) sampling schemes found that stratified random sampling techniques generally yielded smaller variability about population estimates than other random sampling methods. It can be demonstrated mathematically that the variability obtained from stratified random sampling will be smaller than or equal to the variability of random sampling. Through a number of complex mathematical manipulations, the following equation can be derived (Hoel 1971):

$$\sigma^2_{\bar{x}} = \sigma^2_{\bar{x}r} + \sum_{i=1}^s \frac{n_i}{N^2} (\bar{x}_i - \bar{x})^2 \quad (2)$$

where:

$\sigma^2_{\bar{x}}$ is the random sample variance.

$\sigma^2_{\bar{x}r}$ is the stratified sample variance.

n_i is the number of samples for a strata.

N is the total number of samples.

\bar{x}_i is the strata mean.

\bar{x} is the total sample mean.

s is the number of strata.

Since n_i must be +

N must be +

$(x-y)^2$ must be \geq to 0

hence: the sample variance must be \geq stratified variance

The shape and size of the strata have also been studied. It was concluded (Barton, 1956) that the size of the area should be large enough to cover the extent of a parameter in a heterogeneous basin. Accordingly if the area sampled is too small, one would see large differences in variability between the observed sample strata. An arbitrarily large area should also not be selected in as much as it would either decrease the dispersion of the sampling across the basin or increase the sample size and study cost. Reductions in the variability in the estimates will also be affected by the sample area size and shape because the more alike the within-strata parameters are the more effective the stratified sampling (Snedecor and Cochran, 1967). The appropriate strata area size or shape for geological studies is unknown and may change from parameter to parameter.

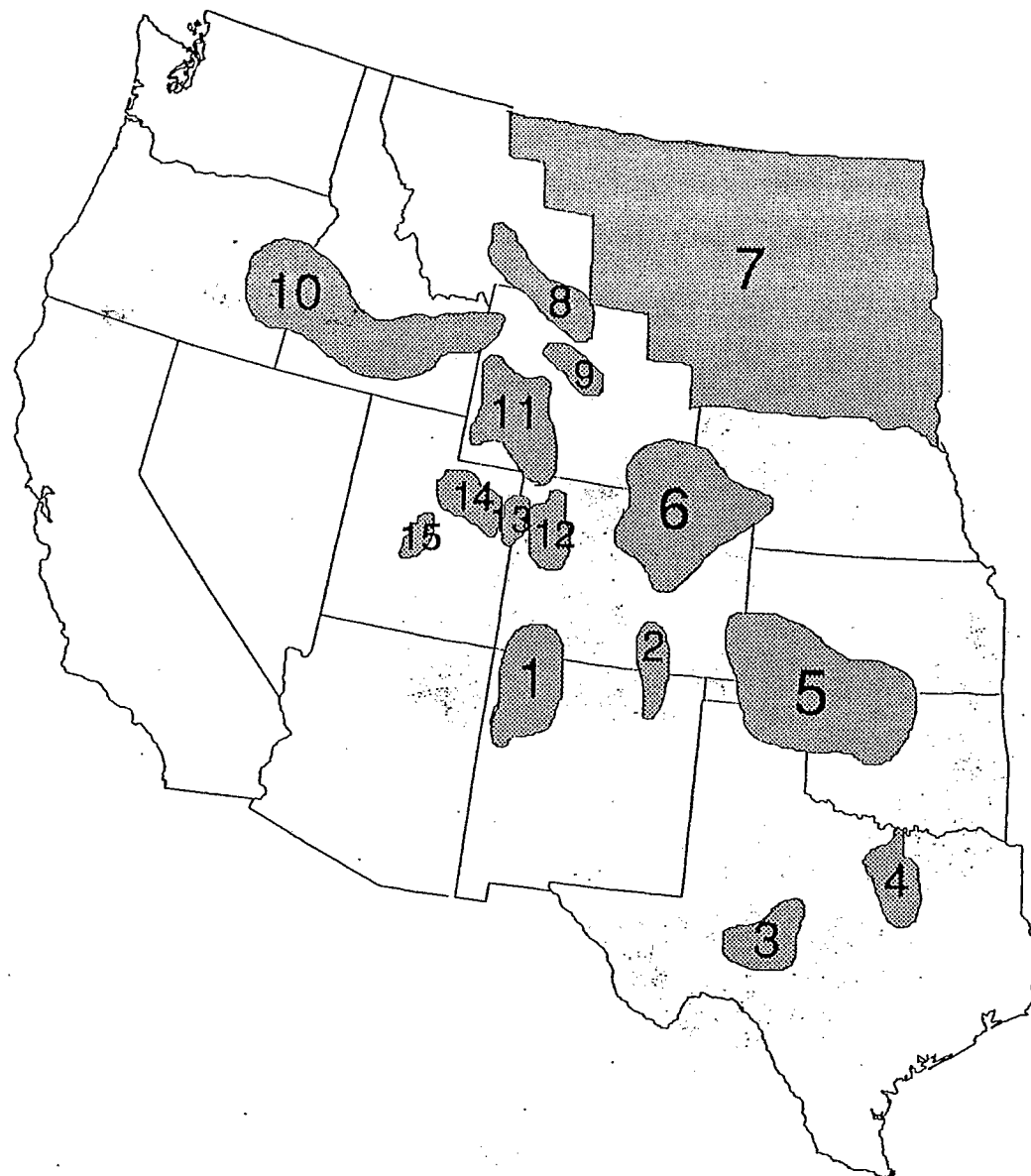
Based upon review of similar studies it seemed reasonable to assume that the precision of a hydrocarbon resource/reserve evaluation can be efficiently estimated with stratified random sampling techniques. This study compares the variability obtained using stratified sampling techniques with the variability of simple random sampling, and examines the effect of the areal size of a strata.

II. APPLICATION OF TECHNIQUE TO THE DAKOTA FORMATION OF THE SAN JUAN BASIN

The San Juan Basin (Figure 1) of northwestern New Mexico and southwest Colorado is one of several structural basins formed in the Rocky Mountain region during the Late Cretaceous to Eocene Laramide orogeny. The present outline (Figure 2) of the basin comprises approximately 8000 square miles and is roughly defined by the outcrop of the contact of the Upper Cretaceous Pictured Cliffs Sandstone and the overlying Fruitland Formation.

The Dakota Formation was deposited during an early stage of the initial transgression of the Cretaceous Western Interior Seaway. Its base consists of non-marine rocks which grade upward to marine beach and offshore bars (Hoppe, 1978). Permeability and porosity are usually low so that the formation is considered to be a tight, blanket sandstone. Most of the gas is trapped stratigraphically in the upper sandstone layers with the lower non-marine section being predominantly water bearing. There are some structural traps in the Dakota in the Colorado portion of the basin (Hoppe, 1978).

In 1980 the NPC did an in place gas estimate for the Dakota Formation in an area of the San Juan Basin (Figure 2). They outlined the current productive area and delineated an area around the productive area that they believed would ultimately be productive. Within the ultimately productive area they estimated reservoir parameters such as net pay and gas filled porosity and used those estimates to calculate gas-in-place. This study sampled wells from the 1980 current productive area.



1. SAN JUAN BASIN
2. RATON BASIN
3. VAL VERDE BASIN
4. FORT WORTH BASIN
5. ANADARKO BASIN
6. DENVER BASIN
7. NORTHERN GREAT PLAINS PROVINCE
8. BIG HORN BASIN
9. WIND RIVER BASIN
10. SNAKE RIVER DOWNWARP
11. GREATER GREEN RIVER BASIN
12. PICEANCE BASIN
13. DOUGLAS CREEK ARCH
14. UINTA BASIN
15. WASATCH PLATEAU

Figure 1. Index map of western U.S. showing location of San Juan Basin
(Modified from GRI 1982).

- APPROXIMATE DAKOTA PRODUCING AREA - 1980
- ▨ APPROXIMATE ULTIMATE DAKOTA PRODUCING AREA - NPC 1980
- SAMPLED TOWNSHIPS

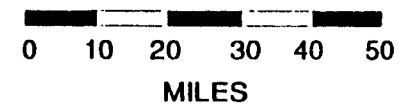
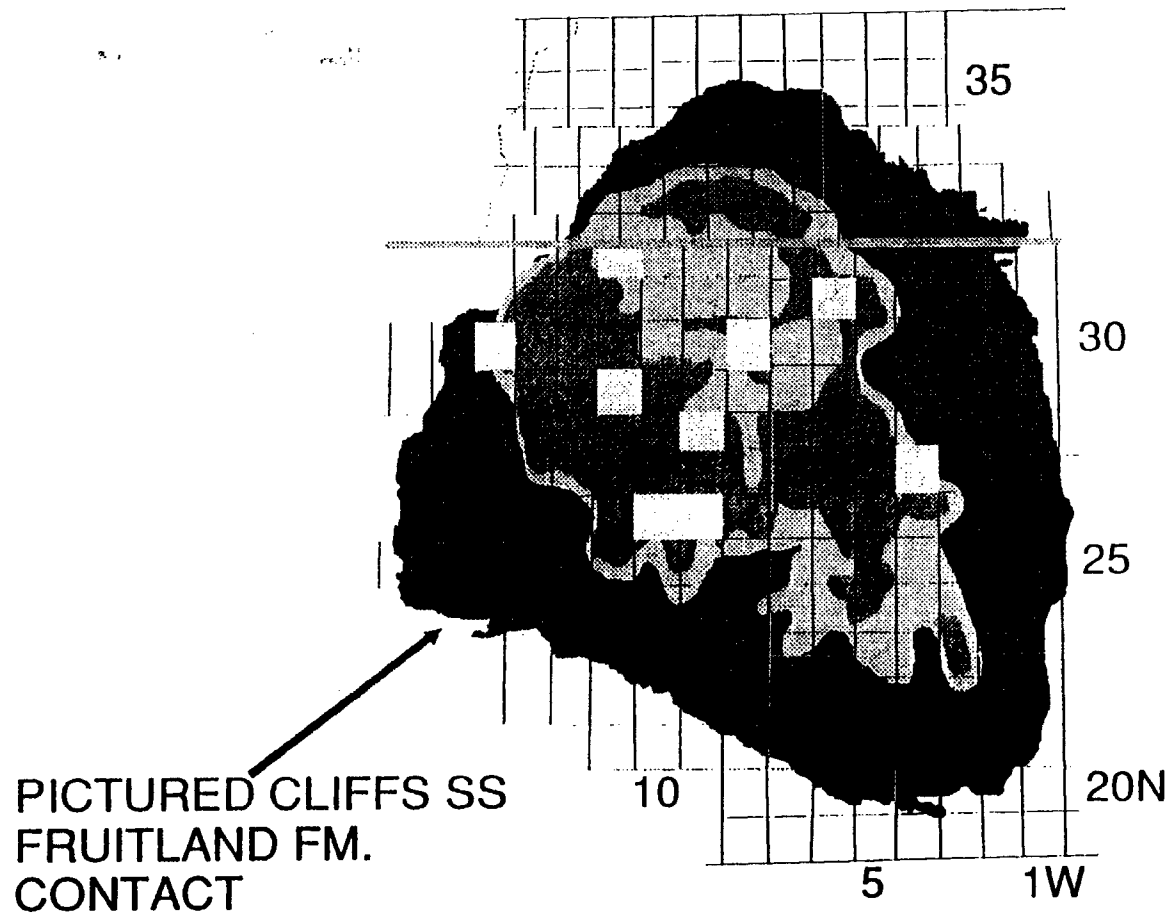


Figure 2. Map of San Juan Basin

The data sampling was conducted by listing all the townships partially or totally included in the producing area as determined by the NPC (NPC,1980). Twelve townships were randomly selected from the list (Table 1). Figures 2 and 3 depict the location of the selected townships. Nine sections were chosen from each of the selected townships (Table 1). The selection of these nine sections was done by randomly selecting a start number from 1 to 4 and then choosing each fourth section after the start number. All the wells in the 1986 version of the Well History Control System (WHCS) of Petroleum Information Corporation (PI) which were drilled in the selected sections and which penetrated the Dakota were identified and the electronic well logs for these wells were acquired from PI.

TABLE ONE
Randomly Selected Strata

Township Range	Start Section	Selected Sections
* Twn26-N Rge04-W	3	3,7,11,15,19,23,27,31,35
Twn26-N Rge09-W	1	1,5,9,13,17,21,25,29,33
Twn26-N Rge10-W	1	"
Twn27-N Rge04-W	3	3,7,11,15,19,23,27,31,35
Twn28-N Rge09-W	4	4,8,12,16,20,24,28,32,36
Twn29-N Rge11-W	1	1,5,9,13,17,21,25,29,33
Twn30-N Rge08-W	2	2,6,10,14,18,22,26,30,34
Twn30-N Rge14-W	4	4,8,12,16,20,24,28,32,36
* Twn31-N Rge06-W	4	"
Twn32-N Rge06-W	4	"
Twn32-N Rge11-W	2	2,6,10,14,18,22,26,30,34
Twn33-N Rge10-W	1	1,5,9,13,17,21,25,29,33

* No wells with logs were available from these border townships

III. PARAMETER ESTIMATION

The Dakota Formation tops and bottoms were picked on the well logs and the picked intervals were then digitized and entered into the ESLog well log analysis system by a data entry clerk while under the supervision of a geologist. ESLog is a commercial software system developed by Energy Systems Inc. of Denver Colorado which helps analyze well log data. Producing zones in the Dakota Formation were obtained for each well by examining the perforation records in the WHCS (Well History Control System). The WHCS is a data base created by Petroleum Information Inc. which contains information on more than 1.8 million wells drilled in the United States. Three zones of sand were recognized within the Dakota interval. In nearly all wells, the upper two zones observed on the logs were perforated, while the lower zone, which was usually wet, was only perforated in a few wells. Since nearly all wells examined had perforations in both upper zones, these two sands were grouped together for this study and the lower zone was not examined in detail.

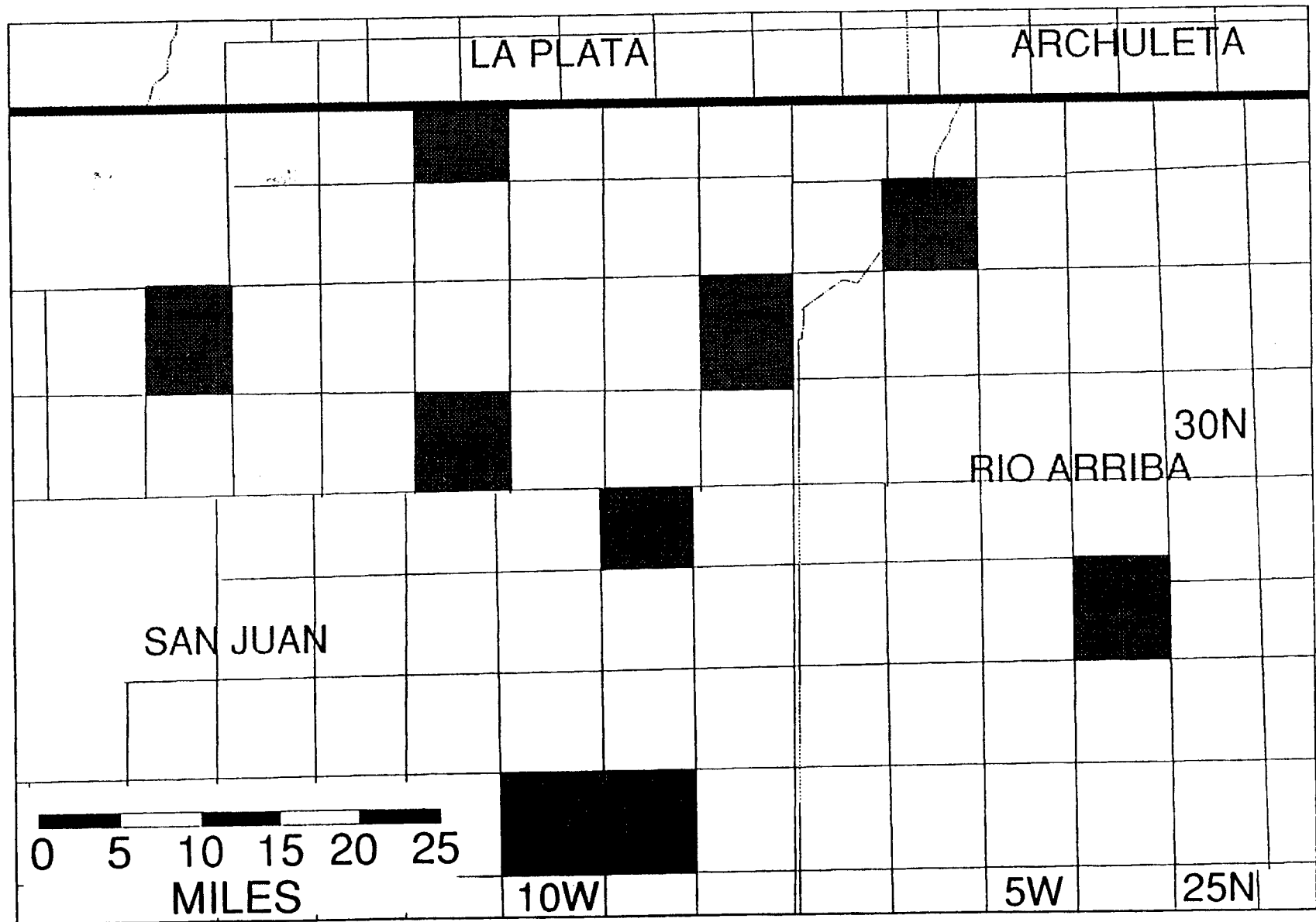


Figure 3. Townships selected for study showing wells sampled from these townships

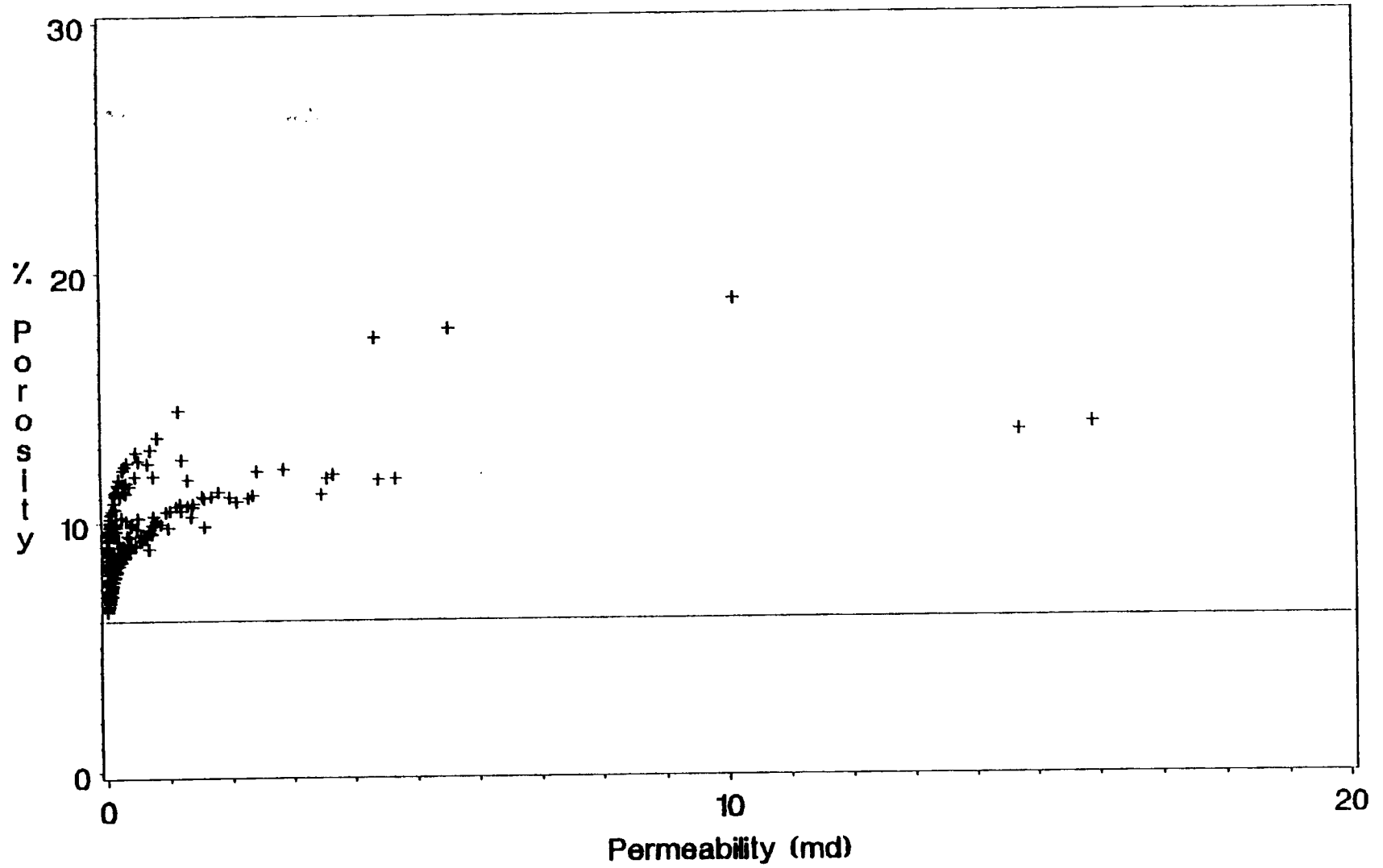
Gamma ray, spontaneous potential, deep induction, short normal resistivity, sonic, neutron, bulk density, and density porosity curves were digitized. The ESLog single porosity model was used to calculate porosity, water saturation, and permeability indices for the Dakota sands in each well at a .5 foot interval. Input required for the single porosity model includes the following:

- . neutron porosity (CNL or SNP), or density (bulk density or density porosity), or sonic
- . true resistivity (deep reading)

The Archie equation was used to calculate water saturation. The water resistivity used was .1 ohm-m, which is the default of the ESLog system; the actual formation resistivity values were not used. The gross Dakota sand thickness was determined from log picks of the top and bottom of the Dakota formation. Net sand thickness was determined by eliminating the Dakota sands with permeabilities lower than .004 md. Whenever permeability exceeded .004 md and porosity was less than 6 percent the original and the digitized log traces were checked for accuracy. In some instances ESLog calculated unreasonably high permeability values. Any permeability value greater than 20 md was flagged and the associated traces checked for accuracy. All but eight half-foot permeability readings of the high permeability values were attributed to poor original trace data, digitizing errors, and well wash out. The poor well traces were reviewed and a subjective estimate as to gas producing ability of the sands was made by the geologist.

Since some area operators use 6 percent as a porosity cutoff for this formation, porosity values were compared to their associated permeability values. A plot of porosity versus permeability (Figure 4) clearly shows that the results of this study would be virtually identical using either a porosity cutoff of 6 percent or a permeability cutoff of .004 md. The Dakota sand which exceeded the cutoff value was judged producible and summed to yield a net sand thickness for each well. The porosity, permeability and water saturation values from the producible intervals in each well were analyzed for their statistical distributional properties. Most of the distribution for the porosity and water saturation for each of the 63 wells typically exhibited normal distributions, while the permeabilities exhibited log normal distributions (Figure 5). These are the distributions typically displayed by these parameters. The porosity and water saturation normal means were calculated for each well as was the log-normal permeability mean. These values were then used to calculate the average values for each township and range listed in Table 2.

Plot of Porosity Versus Permeability



-382-

FIGURE 4 data from four wells displayed

Example Well Permeability Distribution

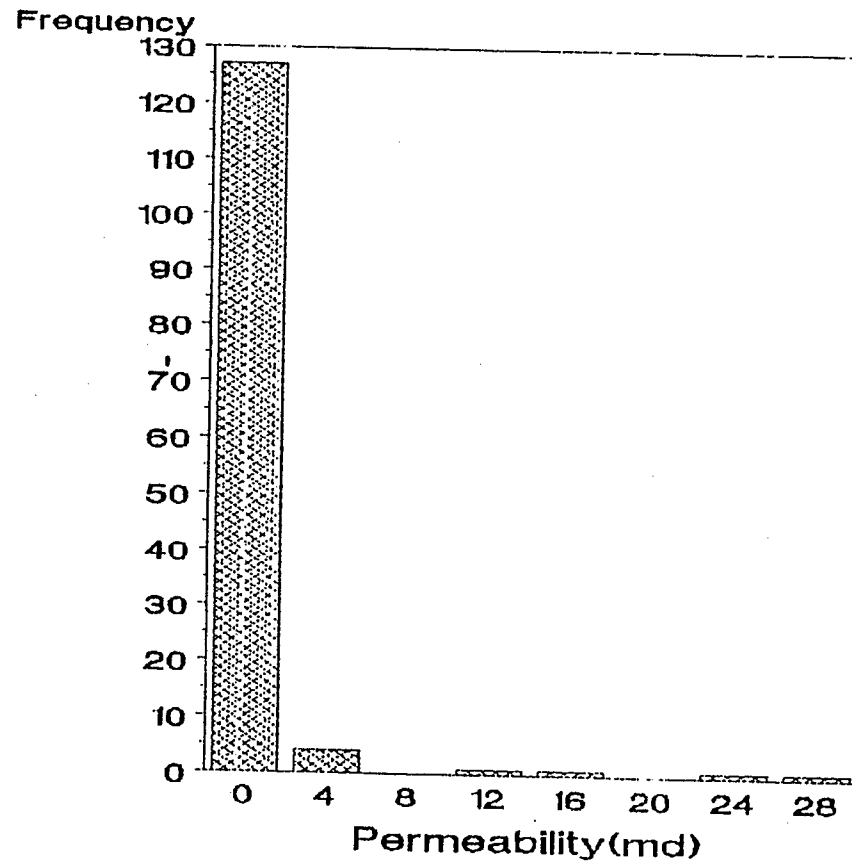


FIGURE 5

TABLE TWO.
MEAN VALUE PER TOWNSHIP *

	MEAN POROSITY (PERCENT)	MEAN WATER SATURATION (PERCENT)	MEAN NET SAND (FEET)	MEAN PERMEABILITY INDEX (MD)	NUMBER OF WELLS SAMPLED
26N 9W	8.11	26.57	23.00	0.17	13
26N 10W	9.49	32.59	28.29	0.08	10
27N 4W	17.62	19.20	18.58	2.89	5
28N 9W	10.34	29.89	35.61	0.19	9
29N 11W	11.79	27.42	31.81	.36	13
30N 8W	15.21	21.40	35.50	.60	2
30N 14W	12.34	34.31	7.75	1.11	2
31N 6W	13.45	21.23	30.66	.53	6
32N 11W	14.98	22.45	28.00	.65	2
33N 10W	18.48	16.06	66.00	1.02	1
ALL WELLS	11.41	26.94	28.43	.5	63

IV. STATISTICAL DETERMINATIONS

The means of each parameter for each section was calculated (Table 3 Appendix). Each section was weighted as to its strata's area proportion of the total area sampled. Standard stratified statistical procedures (Vries, 1986, Snedecor and Cochran, 1967), and simple random statistic procedures (Snedecor and Cochran, 1967) were applied to the data in Table 3. The statistically derived means of the studied parameters and the 95% confidence range for these means are presented in Table 4. The 95% confidence range is the range that the true value of the reservoir parameters, as measured in this study, will fall within 95 percent of the time. That is, we are 95% sure that the true net sand mean value, as measured by electronic logs, falls between the upper (35.94 ft) and lower (21.72 ft) confidence bounds.

TABLE FOUR
PARAMETER ESTIMATES FOR PRODUCING AREA OF FIGURE 2

Parameter	STRATIFIED SAMPLING			RANDOM SAMPLING		
	Lower 95% Limit	Weighted Mean	Upper 95% Limit	Lower 95% Limit	Weighted Mean	Upper 95% Limit
Permeability (MD)	.092	.142	.266	.060	.142	.349
Porosity (Percent)	10.38	12.14	13.90	10.05	12.14	14.22
Percent Water Saturation	21.38	25.78	30.46	21.30	25.78	30.54
Net Sand Thickness(ft)	21.72	28.82	35.94	21.38	28.82	36.62

∇ COMPARISON WITH NPC(1980) STUDY

By substituting the appropriate numbers Table 4 in Equation 1 an estimate can be made of the cubic feet of gas in place in the Dakota Formation of the ultimate producing area of Figure 2. All other values needed for the gas in place calculation were taken from the NPC report. They are:

- z= .91
- T= 682 degrees Rankin
- P= 3,090 pounds per square inch atmospheric
- A= 1,188 square miles

The values for water saturation from Table 4 were not used in equation 1 since they are known to be in error due to the fact the correct formation water resistivity was not used to derive them. From data given by Hoppe (1978) the formation water resistivity should be approximately .8 ohm-m. The average values of water saturation were adjusted using the .8 water resistivity value, and are presented in Table 5. The gas-in-place figures for the ultimate producing area should be considered optimistic since they are based on rock parameters from the productive area and the NPC (1980) felt that rock quality would deteriorate in the ultimate producing area.

Estimates of the 95% confidence range were also made for these values by substituting the upper and lower limit values of the appropriate parameters. (These limits are conservative since the likelihood of all three of the parameters being at the lower 95% limit of their estimate is less than 5%). These values are reported in Table 5.

TABLE FIVE
CALCULATED ESTIMATES FOR ULTIMATE PRODUCTIVE AREA OF FIGURE 2

Parameter	Lower 95% Limit	Weighted Mean	Upper 95% Limit
Water Saturation (%)	56.27	75.8	80.78
* Gas Filled Porosity (%)	1.7	2.9	6.5
Gas In Place (BCF)	2,253	4,955	9,157

* Gas filled porosity is the porosity multiplied by (1 - the water saturation)

6. RESULTS/ACCOMPLISHMENTS:

As explained in the following paragraphs it is concluded that stratified random sampling does reduce variability in parameter estimates and that the NPC (1980) estimate of gas-in-place in the ultimately productive area of figure 2 was reasonable.

I. Verification of the NPC Study

At the outset of this study it was decided to verify the reservoir parameters such as gas-filled porosity and net pay thickness used by the NPC (NPC,1980) to calculate in-place gas reserves for an area in the San Juan Basin. By a method not stated, but probably by taking the opinions of experts, the NPC (NPC,1980) predicted that reservoir parameters in the Dakota Formation for the ultimately productive area would be of lower quality than for the productive area in 1980. The NPC (NPC,1980) stated that in the productive area the net pay was 50 to 70 feet thick, the average porosity was 8%, and the water saturation varied from 30 to 50%. They estimated that in the ultimately productive area gas-filled porosity values would range from 1.5% to 5% and net pay thickness would range from 10 to 30 feet. Using the volumetrics equation (Equation 1), the NPC calculated a value of 3.298 TCF gas-in-place of which they estimated that 2.213 TCF (67%) was recoverable.

The estimates of ranges for porosity (10.38% to 13.90%) and net sand thickness (21.72 ft to 35.94 ft) are different (the NPC porosity is less, the NPC net sand is greater) than the NPC (1980) estimates for the producing area. Also, the range for adjusted water saturation (56.27% to 80.78%) in Table 5 is less than the NPC (1980) value. The parameter estimates given in Table 4 and table 5 are statistically meaningful and are probably more accurate than the NPC (1980) values which are the opinions of experts.

When the values for net pay and porosity given in Tables 4 and the water saturations from Table 5 are used in equation 1 the differences between this study and the NPC (1980) appear to approximately cancel out. The in-place gas estimate of 3.298 TCF of the NPC (1980) falls within the 95% confidence bounds of this study and is also less than the mean of 4.955 TCF which was an optimistic estimate based on the good rock parameters in the 1980 producing area. It is concluded therefore that the NPC estimate is quite reasonable.

II. Effectiveness of the Stratified Random Sample

A comparison of the two sampling methods, random and stratified, shows a decrease in the stratified methods variability for every parameter studied. The largest decrease is evident in the permeability calculations where the stratified samples confidence range is 35% smaller than the confidence range of the random sample $(1.00 - (.266-.078)/(.349-.06) = .35)$. Less impressive gains are exhibited with the other parameters. For instance the same calculation yields a 9% decrease in the gas-in-place confidence range.

The random stratification did reduce the variability of the estimates with a negligible time and resource investment. The technique would probably be more effective if the sampled sections were grouped closer together. For instance if the center section and its 8 adjacent sections were grouped as a strata instead of the every fourth block in the township the variability would probably be further reduced (Figure 6). In addition to requiring little additional resources the stratified sampling method also allows an in-depth study of small sub areas of the population. This seems to coincide nicely with the fact that geologists often study small areas of a large basin. Based on these results the predicted number of section which would need to be sampled to obtain a given confidence range for porosity is presented in Table 6.

TABLE SIX
Estimated Sample Size Needed to
Obtain a Given Confidence Range

Number of Sections	Confidence Range (upper 95%- lower 95%)
20	3.40% (porosity + or - 1.70%)
40	2.30% (porosity + or - 1.65%)
50	2.03% (porosity + or - 1.0%)
75	1.56% (porosity + or - 0.8%)

To obtain correct gas-in-place estimates for the area studied accurate measurements for values such as water resistivity must be obtained and used in deriving parameter estimates so that correct parameter values can be used in Equation 1. Whenever possible the parameters derived from logs should be verified with core and drill stem test data.

CURRENT STUDY

6	5	4	3	2	1
7	8	9	10	11	12
18	17	16	15	14	13
19	20	21	22	23	24
30	29	28	27	26	25
31	32	33	34	35	36

RECOMMENDED

6	5	4	3	2	1
7	8	9	10	11	12
18	17	16	15	14	13
19	20	21	22	23	24
30	29	28	27	26	25
31	32	33	34	35	36

Figure 6

7. FUTURE WORK:

Because stratified random sampling has been shown to give improved estimates of reservoir parameters used in hydrocarbon reserve calculations it will be employed in the future to select wells for gas-in-place estimates of the Douglas Creek Arch of northwest Colorado. It also may be used in some areas of the Green River Basin as well.

The method does not have to be limited to a volumetrics equation of gas reserves. It could be employed to choose producing wells from a large field to perform decline curve analyses on each and then determine average reserves per well, or in any other process were the size of the study population precludes studying all available data.

8. REFERENCES:

- Bourdeau, Philippe F. 1953, "A Test of Random Verses Systematic Ecological Sampling", Ecology 34 i, pp 474-487
- Hoel, Paul G., 1971. Introduction to Mathematical Statistics, John Wiley & Sons, New York
- Hoppe, W.F., 1978. Basin Dakota Field. Oil and Gas Fields of the Four Corners Area, Four Corners Geological Society, pp 204-206
- Husch, Bertram, 1971. "Planning A Forest Inventory", Food and Agricultural Organization of The United Nations
- National Petroleum Council, 1980. Tight Gas Reservoirs, Volume V, Part II. Unconventional Gas Sources, Committee on Unconventional Gas Sources, John Bookout, Chairman
- Snedecor, George W. and Cochran, William G., 1967. Statistical Methods, Iowa state Univ. Press
- Vries, Pieter G., 1986, Sampling Theory for Forest Inventory, Spninser, Verlag. Berlin

9. APPENDIX:

TABLE 3
Section Values Used For statistical Calculations

SEC	TOWNSHIP	NETSAND	SEC WEIGHT	STRATA WEIGHT	POR%	K md	WATER SATURATION	STRATA WEIGHT
01	26-N 10-W	47.6667	6	36	9.6267	-2.8267	30.9132	0.0260870
01	29-N 11-W	15.3333	6	30	13.3637	-1.6751	28.6384	0.0217391
02	30-N 08-W	12.5000	2	20	11.5940	-1.3816	25.3872	0.0434783
03	27-N 04-W	33.5000	4	26	8.1328	-3.3214	26.4824	0.0282609
05	26-N 09-W	1.0000	5	34	2.5096	-5.9982	26.9152	0.0295652
05	26-N 10-W	14.0000	6	36	8.9768	-2.7694	25.5948	0.0260870
06	30-N 08-W	58.5000	2	20	18.8442	-0.0429	17.4199	0.0434783
07	27-N 04-W	25.0000	4	26	16.6490	0.7072	10.9680	0.0282609
09	26-N 09-W	27.0000	5	34	8.4224	-2.9395	22.5854	0.0295652
09	26-N 10-W	19.2500	6	36	10.4856	-2.6315	36.0080	0.0260870
12	28-N 09-W	37.5000	6	30	9.3689	-1.3184	7.5886	0.0217391
13	29-N 11-W	35.5000	6	30	9.8945	-1.4956	18.1626	0.0217391
16	31-N 06-W	34.5000	5	34	8.5054	-3.8811	39.3640	0.0295652
17	26-N 09-W	42.2500	5	34	13.8644	-0.8418	21.0429	0.0295652
17	26-N 10-W	21.0000	6	36	9.6657	-3.5205	48.7658	0.0260870
17	29-N 11-W	23.5000	6	30	8.6259	-3.9089	38.1866	0.0217391
19	27-N 04-W	10.5000	4	26	18.9020	-0.5640	23.9027	0.0282609
20	28-N 09-W	17.5000	6	30	10.3184	-2.3895	25.9615	0.0217391
21	26-N 09-W	22.3333	5	34	8.5877	-3.4814	29.9688	0.0295652
21	29-N 11-W	32.2500	6	30	11.4910	-2.0381	29.3921	0.0217391
24	30-N 14-W	7.7500	1	6	12.3403	-2.1072	34.3078	0.0260870
24	31-N 06-W	47.0000	5	34	9.7320	-0.5087	6.9118	0.0295652
25	28-N 09-W	33.5000	6	30	9.7717	-2.9597	31.2693	0.0217391
25	29-N 11-W	41.0000	6	30	15.2063	-1.3419	32.1265	0.0217391
25	33-N 10-W	66.5000	1	4	18.4842	0.0294	16.0640	0.0173913
28	28-N 09-W	32.0000	6	30	9.0025	-3.7029	50.1419	0.0217391
28	31-N 06-W	25.5000	5	34	15.1940	-0.6326	17.1282	0.0295652
29	26-N 09-W	31.7500	5	34	9.5889	-2.9070	32.8465	0.0295652
29	26-N 10-W	33.1667	6	36	8.0907	-3.5603	28.5732	0.0260870
29	29-N 11-W	51.5000	6	30	11.3723	-1.3047	17.4446	0.0217391
30	32-N 11-W	28.0000	1	10	14.9893	-0.5851	22.4571	0.0434783
31	27-N 04-W	16.0000	4	26	25.4920	1.6805	14.2304	0.0282609
32	28-N 09-W	8.0000	6	30	9.2656	-3.2034	31.4721	0.0217391
32	31-N 06-W	24.5000	5	34	17.4115	-0.7784	22.3954	0.0295652
33	26-N 10-W	23.5000	6	36	11.8527	-2.0037	32.0655	0.0260870
36	28-N 09-W	53.3333	6	30	12.1017	-1.5781	24.1539	0.0217391
36	31-N 06-W	26.2500	5	34	14.9356	-1.1315	20.8103	0.0295652